Post-transcriptional silencing of chalcone synthase is involved in phenotypic lability in petals and leaves of bicolor dahlia (Dahlia variabilis) 'Yuino'

AUTHOR(S):

Ohno, Sho; Hori, Wakako; Hosokawa, Munetaka; Tatsuzawa, Fumi; Doi, Motoaki

CITATION:

Ohno, Sho ...[et al]. Post-transcriptional silencing of chalcone synthase is involved in phenotypic lability in petals and leaves of bicolor dahlia (Dahlia variabilis) 'Yuino'. Planta 2018, 247(2): 413-428

ISSUE DATE:

2018-02

URL:

http://hdl.handle.net/2433/231367

Post-transcriptional silencing of *chalcone synthase* is involved in phenotypic lability in petals and leaves of bicolor dahlia (*Dahlia variabilis*) 'Yuino'

Sho Ohno[1]* · Wakako Hori[1] · Munetaka Hosokawa[1] · Fumi Tatsuzawa[2] · Motoaki Doi[1]

[1] *Graduate School of Agriculture, Kyoto University, Sakyo-ku, Kyoto 606-8502, Japan*

[2] *Faculty of Agriculture, Iwate University, Morioka 020-8550, Japan*

*Corresponding author: Sho Ohno

Laboratory of Vegetable and Ornamental Horticulture, Graduate School of Agriculture, Kyoto University, Sakyo-ku, Kyoto 606-8502, Japan

Telephone: +81-75-753-6048, Fax: +81-75-753-6068

E-mail: sohno@kais.kyoto-u.ac.jp

ORCID: orcid.org/0000-0002-0810-0327

Main conclusion

Post-transcriptional gene silencing (PTGS) of a chalcone synthase (*DvCHS2*) occurred in the white part of bicolor petals and flavonoid-poor leaves, however it did not in red petals and flavonoid-rich leaves.

Author contribution

SO and MH conceived the research. SO and MD designed the research. SO, WH and FT conducted the research. SO wrote the manuscript. All authors read and approved the manuscript.

Abstract

Petal color lability is a prominent feature of bicolor dahlia cultivars, and causes plants to produce not only original bicolor petals with colored bases and pure white tips, but also frequently single-colored petals without white tips. In this study, we analysed the molecular mechanisms that are associated with petal color lability using the red-white bicolor cultivar ‘Yuino’. Red single-colored petals lose their white tips as a result of recover of flavonoid biosynthesis. Among flavonoid biosynthetic genes including four chalcone synthase (*CHS*)-like genes (*DvCHS1*, *DvCHS2*, *DvCHS3* and *DvCHS4*), *DvCHS1* and *DvCHS2* had significantly lower expression levels in the white part of bicolor petals than in red petals, while *DvCHS3*, *DvCHS4* and other flavonoid biosynthetic genes had almost the same expression levels. Small RNAs from the white part of a bicolor petal were mapped onto *DvCHS1* and *DvCHS2*, while small RNAs from a red single-coloured petal were not mapped onto any of the four *CHS* genes. A relationship between petal color and leaf flavonoid accumulation has previously been demonstrated, whereby red petal-producing plants accumulate flavonoids in their leaves while bicolor petal-producing plants tend not to. The expression level of *DvCHS2* was down-regulated in flavonoid-poor leaves and small RNAs from flavonoid-poor leaves were mapped onto *DvCHS2,* suggesting that the down-regulation of *DvCHS2* in flavonoid-poor leaves occurs post-transcriptionally. Genomic analysis also suggested that

DvCHS2 is the key gene involved in bicolor formation. Together, these results suggest that post-transcriptional gene silencing of *DvCHS2* plays a key role in phenotypic lability in this bicolor dahlia.

Key words: CHS, flavonoid, flower color, PTGS, siRNA.

Abbreviation

CHS: chalcone synthase

HPLC: high-performance liquid chromatography

PTGS: post-transcriptional gene silencing

SAM: shoot apical meristem

Introduction

Dahlia (*Dahlia variabilis*, Asteraceae) is one of popular floriculture crops that are used as cut flowers and garden plants. Dahlia flowers exhibit huge variations in their traits, including color, shape and size. Flower color is particularly diverse, with purple, red, pink, orange, black, ivory white, yellow, variegated and bicolor cultivars currently available. This huge phenotypic variation may be derived from the complicated genetic background and large genome size of this species, as it is believed to be an autoallooctoploid (Gatt et al. 1998) with a genome that is estimated at more than 8.8 Gb per haploid (Temsch et al. 2008). Due to this complicated genetic background and high heterozygosity, the propagation of dahlias relies on vegetative propagation, such as through tuberous roots and cuttings (Konishi and Inaba 1964).

Bicolor dahlias belong to a group of cultivars that have petals with colored bases and white tips. A prominent feature of these cultivars is the lability, or instability, of petal color, as in addition to the original bicolor petals, they also frequently produce single-colored petals without white tips, despite being propagated vegetatively (Fig. 1). This petal color lability is observed not only among clonal plants but also within a single plant and even within an inflorescence. Bicolor dahlias can bloom inflorescences with only bicolor petals, only single-colored petals, or a mixture of the two. In a mixed inflorescence, the single-colored petals are located in the outer whorls or sectorally in many cases (Ohno et al. 2016), making it unlikely that this phenomenon can be explained by a mutation in particular genes. This petal color lability in bicolor dahlias attracted much research in the 1930s (Lawrence 1931; Tammes and Groeneveld-Huisman 1939) and yet the mechanism(s) underlying it remain unknown.

‘Yuino’ is a red-white bicolor dahlia cultivar that produces petals with red bases

and white tips, but also often produces red single-colored petals (Ohno et al. 2016, Fig. 1). Based on the observation that these red petals occur sectorally in an inflorescence (Ohno et al. 2016), it was assumed that whatever phenomenon controls their production occurs meristematically. There were two types of leaves, one was flavonoid-rich leaves and the other was flavonoid-poor leaves. A relationship between petal color and leaf flavonoid accumulation has been demonstrated, whereby red petal-producing plants tend to produce flavonoid-rich leaves while solely bicolor petal-producing plants tend to produce flavonoid-poor leaves. This indicates that petal color lability can be considered a phenotypic change at the whole-plant level (Ohno et al. 2016).

It has previously been shown that ‘Yuino’ accumulates anthocyanins, flavones and butein in the red parts of the petals, whereas no flavonoids are accumulated in the white tips (Ohno et al. 2011b). The flavonoid biosynthetic genes in dahlia have been largely elucidated, with anthocyanin biosynthesis being regulated by the basic helix-loop-helix transcription factor DvIVS through regulation of the gene expression of chalcone synthase (*DvCHS1*), flavanone 3-hydroxylase, dihydroflavonol 4-reductase, anthocyanidin synthase, anthocyanidin 3-*O*-glucoside-6'-*O*-malonyltransferase and glutathione S-transferase, but not *DvCHS2* and chalcone isomerase (Deguchi et al. 2013; Ohno et al. 2011a, 2013). The flavonoid biosynthetic pathway in dahlia is summarised in Fig. 2. The formation of white tips, i.e. the loss of flavonoids in the white parts of petals, results from simultaneous post-transcriptional gene silencing (PTGS) of two different chalcone synthases, *DvCHS1* and *DvCHS2* (Ohno et al. 2011b). Small RNA of *CHS* was detected from the white tips of a yellow-white bicolor line ‘OriW1’ petals, where *DvCHS1* expression was absent in whole petals, indicated that the PTGS of *DvCHS2* can be induced without *DvCHS1* expression (Ohno et al. 2011b). These results implied that causal gene for PTGS of *CHS* might be *DvCHS2*, however, the genomic background has

not yet been analysed and so the causal gene for simultaneous PTGS of *CHS* remains unknown.

This study had two objectives: to elucidate the underlying mechanism for petal color lability in bicolor dahlia and to identify the causal gene for simultaneous PTGS of *CHS*. We examined this by performing a molecular analysis of labile petals and leaves in 'Yuino', and comparing the red petals with bicolor petals and flavonoid-rich leaves with flavonoid-poor leaves. We also analysed the genomic background of *DvCHS2*, which was silenced in bicolor petals and flavonoid-poor leaves, among bicolor and non-bicolor cultivars.

Materials and Methods

Plant materials

The red-white bicolor dahlia cultivar 'Yuino' (Fig. 1) was used for the experiment. Petals and leaves were collected from field- or greenhouse-grown plants in the experimental field of Kyoto University (Kyoto, Japan) and used in the following analyses. In addition, seven other bicolor cultivars ('Matsuribayashi', 'Kazusa-shiranami', 'Santa Claus', 'OriW1', 'OriW2', 'Shukuhai' and 'Kageboshi') and six single-color cultivars that produce petals without white tips ('Kokucho', 'Ms. Noir', 'Yukino', 'Michael J', 'Fidalgo Blacky' and 'Cupid') were also used in the genomic analysis.

Pigment analysis of petals

Bicolor petals were separated into the outside red area and the inner white area using a razor blade and these parts were collected separately. Red petals were also separated in the same way as bicolor petals and collected. The pigment contents of the different petal

parts were quantified with high-performance liquid chromatography (HPLC). Fresh petal parts were homogenised with a mortar and a pestle under liquid nitrogen, following which 1 mL of extraction solution (5 % hydrochloric acid in 50 % methanol) was added. The mixture was then centrifuged at 4°C at 15,000 rpm for 15 min, and the supernatant was collected and diluted 50 times with the same solvent. For hydrolysis, 1.2 mL of the diluted solution was boiled at 95°C for 2 h and 20 µL of the hydrolysed solution was injected into the HPLC apparatus. The analysis was performed using an HPLC system (Hitachi L-7100, L-7200, L-7420, L-7500; Hitachi Systems, Ltd., Tokyo, Japan) with a C18 column (Nihon Waters K.K., Tokyo, Japan) that was maintained at 40°C. The detection wavelength was 350 nm for flavones and chalcones, and 520 nm for anthocyanidins. Eluant preparation and HPLC analysis proceeded according to Ohno et al. (2011b). The assay was performed with six different petals.

Isolation of new CHS *homologs*

A partial sequence of *DvCHS3* (JN556044) was obtained from NCBI database and a partial sequence of *DvCHS4* was obtained from transcriptome data (unpublished data) composed for ‘Yuino’, ‘Michael J’ and ‘Kokucho’ petals, and SRR797209 (Hodgins et al. 2014). The rapid amplification of cDNA 3′ and 5′ ends was performed using a library constructed with the GeneRacer™ Kit (Invitrogen, Carlsbad, CA, USA) of ‘Michael J’ (Ohno et al. 2011a). Primers for full-length cDNAs, genome sequencing and real-time RT-PCR were designed (Table S1) and sequenced using ‘Yuino’ petal RNA and genomic DNA. Sequencing analysis was performed using a BigDye® Terminator v 3.1 Cycle Sequencing Kit and a 3100 Genetic Analyzer (Applied Biosystems, Foster City, CA, USA).

176 *Phylogenetic analysis*

177 A phylogenetic tree was constructed based on the open reading frames or amino acids of
178 various *CHS* genes and several other polyketide synthase genes using the Neighbor-
179 Joining method (Saitou and Nei 1987).

180 The accession numbers for the DNA sequences were as follows: *DvCHS1-1*
181 (AB576660), *DvCHS1-2* (AB576661), *DvCHS2-1* (AB591825), *DvCHS2-2* (AB591826),
182 *DvCHS3-1* (LC223139), *DvCHS3-2* (LC223140) and *DvCHS4* (LC223141) in *D.*
183 *variabilis*; *AmCHS1* (X03710) in *Antirrhinum majus*; *AtTT4* (NM_121396) in
184 *Arabidopsis thaliana*; *GhCHS1* (Z38096), *Gh2PS* (Z38097), *GhCHS3* (Z38098) and
185 *GhCHS4* (AM906210) in *Gerbera hybrida*; *GmCHS3* (FJ770471) and *GmCHS7*
186 (AK245977) in *Glycine max*; *InCHSD* (AB001818) and *InCHSE* (AB001819) in *Ipomoea*
187 *nil*; *MsCHS1* (L02901) in *Medicago sativa*; *PhCHSA* (AF233638) and *PhCHSJ* (X14597)
188 in *Petunia hybrida*; *VvCHS1* (EF192464), *VvCHS3* (AB066274) and *VINST1*
189 (NM_001281010) in *Vitis vinifera*; and *ZmWHP* (X60204) in *Zea mays*.

190 The accession numbers for the amino acid sequences were as follows: DvCHS1-
191 1 (BAJ14768), DvCHS1-2 (BAJ14769), DvCHS2-1 (BAJ21531), DvCHS2-2
192 (BAJ21532), DvCHS3-1 (BAX02592), DvCHS3-2 (BAX02593) and DvCHS4
193 (BAX02594) in *Dahlia variabilis*; AtTT4 (NP_196897.1) in *Arabidopsis thaliana*;
194 GhCHS1 (CAA86218), GhCHS3 (CAA86220) and GhCHS4 (CAP20328) in *Gerbera*
195 *hybrida*; GmCHS3 (ACN81822) in *Glycine max*; InCHSD (BAA21787) and InCHSE
196 (BAA21788) in *Ipomoea nil*; and PhCHSA (AAF60297) and PhCHSJ (CAA32737) in
197 *Petunia hybrida*. The amino acid sequence of GmCHS7 was estimated from AK245977.
198
199 *Real-time RT-PCR*
200 To analyse petal flavonoid biosynthetic gene expression, bicolor petals were separated

into the colored outer part and the pure white inner part, and RNA was extracted from each. Red single-colored petals were also separated into the same parts and RNA was extracted from each of these. Unfolded bicolor and red petals were collected from the same region of the same inflorescence, with pairs of petals being collected from three different inflorescences. To analyse leaf flavonoid biosynthetic gene expression, we obtained six 3-5 cm leaves with or without flavonoid accumulation, as determined from their ABS_{400}/ABS_{370} scores measured by a spectrophotometer according to Ohno et al. (2016): leaves with a score >0.8 were judged to have accumulated an abundance of flavonoids, while leaves with scores <0.5 were judged to have accumulated fewer flavonoids. The ABS_{400}/ABS_{370} scores were 1.005, 0.976, 0.969, 0.955, 0.925 and 0.922 in flavonoid-rich leaves, compared with 0.344, 0.269, 0.264, 0.192, 0.178 and 0.114 in flavonoid-poor leaves.

Total RNA was extracted from petals and leaves using Sepasol RNA I Super G (Nacalai Tesque, Kyoto, Japan), purified with a high-salt solution for precipitation (Takara Bio Inc., Ohtsu, Japan) and reverse transcribed with ReverTra Ace® (Toyobo, Osaka, Japan), following which 2 µL of 50-fold diluted RT product was used as a template for real-time RT-PCR. Real-time RT-PCR was performed with SYBR® Premix Ex Taq™ II (Takara Bio Inc.) according to the manufacturer's instructions using the LightCycler® 480 system (Roche Diagnostics K.K., Tokyo, Japan). The real-time RT-PCR was performed as follows: 95°C for 5 min, followed by 45 cycles at 95°C for 10 s and 60°C for 30 s. Single-target product amplification was checked using a melting curve. The primers that were used for real-time RT-PCR are shown in Table S2.

Protein extraction and western blotting

Total protein from petals was extracted using Minute Total Protein Extraction Kit for

Plant Tissues (Invent Biotechnologies Inc., Eden Prairie, MN). Total protein from leaves was extracted according to the method of Wang et al. (2010) with minor modification. Briefly, 2 g of leaf was ground to a fine powder under liquid nitrogen and then 6 mL extraction solution was added. The extraction solution consisted of 50 mM Tris-HCl (pH 9.0), 2% SDS, 5 mM ascorbic acid, 14 mM β-mercaptoethanol and 1% proteinase inhibitor cocktail for plant cell and tissue extracts, DMSO solution (SIGMA-ALDRICH Co., St. Louis, MO). The homogenate was filtered through 4 layers of Miracloth (Millipore, Billerica, MA) and centrifuged at 4°C at 15,000 rpm for 20 min. The supernatant was used as the total protein. Protein concentration was determined by Protein Quantification Kit-Rapid (Dojindo, Kumamoto, Japan). To determine flavonoid accumulation, 100-200 mg of leaf were collected from the same leaf or the same branch of protein extracted leaves. The ABS_{400}/ABS_{370} scores for flavonoid-rich leaves were 1.000, 0.992 and 0.965, while 0.158, 0.120 and 0.252 for flavonoid-poor leaves.

For western blotting analyses, 10 μg of total proteins in the sodium dodecyl sulfate polyacrylamide gel electrophoresis gel (the concentration for running gel was 8% and for stacking gel was 3%) were transferred to an Immobilon-P membrane (Millipore). The blots were probed with 1:2000 dilution of the primary anti-GmCHS7 peptide (NH2-C+FRGPSDTHLDSLVGQ –COOH) IgG (rabbit) and 1 : 20000 dilution of the secondary goat Anti-rabbit IgG, HRP-linked Antibody (Cell Signalling Technology, Danvers, MA). The immune complexes were visualized by a peroxidase-catalyzed chemiluminescence reaction using an ECL Western blotting kit (GE Healthcare Japan, Tokyo, Japan) following the manufacturer's instructions. The chemiluminescence image was obtained using a LAS-3000 Mini (Fujifilm, Tokyo, Japan). For positive control, the *DvCHS2-1* coding sequence was subcloned into pET6xHN-C vector, and the *DvCHS2*-His fusion protein was expressed in *E. coli* and purified via His60 Ni gravity column using pET

Express & Purify Kit-His60 (In-Fusion® Ready) (Takara Bio inc.). Primers used for constructing *DvCHS2*-His fusion protein were pET-6xHN-C-DvCHS2-F: 5′-TAAGGCCTCTGTCGAGATGGCATCTTCGGTCGATA-3′ (forward) and pET-6xHN-C-DvCHS2-R: 5′-CAGAATTCGCAAGCTTGGGCGAAATCGGCATGGTA-3′ (reverse).

Analyses of small RNAs

The detection of *CHS* siRNA by RNA gel blot analysis was performed according to Ohno et al. (2011b). The ABS_{400}/ABS_{370} scores of leaves used for RNA extraction were 0.907, 0.795 and 0.934 for flavonoid-rich leaves, and 0.200, 0.101 and 0.050 for flavonoid-poor leaves.

For the mapping analysis of petals, small RNAs were extracted from a 5-cm expanded red petal using the MirVana miRNA Isolation Kit (Applied Biosystems) according to the manufacturer's instructions. Small RNAs were sequenced using an Illumina Hiseq (Illumina Inc., San Diego, CA, USA), and 18–32 nt small RNAs were mapped onto *DvCHS* genes (*DvCHS1-1*, *DvCHS1-2*, *DvCHS2-1*, *DvCHS2-2*, *DvCHS3-1*, *DvCHS3-2* and *DvCHS4*) using the Bowtie software without any mismatch. The number of total reads for a red petal was 13,681,764. For the white part of a bicolor petal, previous small RNA data (Ohno et al. 2011b) were used and newly mapped onto *DvCHS3-1*, *DvCHS3-2* and *DvCHS4*.

For the mapping analysis of leaves, small RNAs were extracted from a flavonoid-rich leaf and a flavonoid-poor leaf using the MirVana miRNA Isolation Kit (Applied Biosystems) according to the manufacturer's instructions. Each leaf was separated along the midrib using a razor, and one half was used for spectrophotometric measurement and HPLC analysis while the other half was used for RNA extraction. The

276 ABS_{400}/ABS_{370} scores were 0.969 and 0.178 for the flavonoid-rich and flavonoid-poor
277 leaves, respectively, and flavonoid accumulation was confirmed by HPLC. A small RNA-
278 enriched sample was used for the small RNA mapping analysis and the rest of the RNA
279 fraction that was depleted of small RNAs was used for the RNA-seq analysis described
280 below. Small RNAs were sequenced using an Illumina Hiseq (Illumina Inc.) and 18–30
281 nt small RNAs were mapped onto *DvCHS* genes (*DvCHS1-1*, *DvCHS1-2*, *DvCHS2-1*,
282 *DvCHS2-2*, *DvCHS3-1*, *DvCHS3-2* and *DvCHS4*) using the Bowtie software without any
283 mismatch. The number of total reads was 12,046,092 for a flavonoid-rich leaf and
284 11,465,948 for a flavonoid-poor leaf.
285
286 *RNA-seq analysis*
287 RNA-seq analysis was performed with the HiSeq2000 sequencing system (Illumina)
288 using the RNA fraction that had been depleted of small RNAs from the rest of small RNA
289 mapping analysis. The number of total reads was 4,059,802 for a flavonoid-rich leaf and
290 4,579,744 for a flavonoid-poor leaf. The differentially expressed genes between these
291 samples were evaluated using edgeR (Robinson *et al.*, 2010) with a border value of logFC
292 = 3 and were confirmed by RT-PCR.
293
294 *DNA gel blot analysis*
295 Genomic DNA was extracted from leaves of bicolor and single-color cultivars using
296 MagExtractor® Plant Genome (Toyobo). A 20-μg DNA sample was digested with a
297 restriction enzyme (*Bam*HI or *Hin*dIII) and separated on 0.8 % agarose gel in 0.5 ×TAE
298 buffer, and subsequently blotted to a Hybond-N+ membrane (GE Healthcare Japan) in 20
299 ×SSC buffer. For the probe, the PCR product was purified from agarose gel slices with
300 the illustra™ GFX™ PCR DNA and Gel Band Purification Kit (GE Healthcare Japan),

and labelled with the AlkPhos Direct Labelling and Detection System (GE Healthcare Japan). The probe was hybridised to the membrane at 55 ºC overnight. Detection was conducted with CDP-Star® (GE Healthcare) and the chemiluminescence image was obtained using a LAS-3000 Mini (Fujifilm).

Inverse and allele-specific PCR

To isolate unknown genomic region, inverse PCR was performed. Genomic DNA of 'Yuino' and 'Michael J' was digested with a restriction enzyme (*Bam*HI, *Hin*dIII or *Xba*I). A 300-ng digested DNA sample was then self-ligated by T4 DNA ligase (Takara Bio Inc.) in a 200-μL volume. Inverse PCR was performed with Blend Taq (Toyobo) or Takara EX Taq (Takara Bio Inc.). To analyse allele composition, allele-specific PCR was performed. For allele-specific PCR, genomic DNA extracted using MagExtractor -Plant Genome- (Toyobo) from leaves of six bicolor cultivars ('Yuino', 'Matsuribayashi', 'Kazusa-shiranami', 'Santa Claus', 'OriW1' and 'OriW2') and four single-color cultivars ('Kokucho', 'Ms. Noir', 'Yukino' and 'Michael J') was used. The primers that were used for inverse PCR, sequencing and allele-specific PCR analysis are shown in Table S3.

Quantification of the genomic region of DvCHS1 *and* DvCHS2

Genomic DNA was extracted from leaves of four bicolor cultivars ('Yuino', 'Shukuhai', 'Kazusa-shiranami' and 'Kageboshi') and four single-color cultivars ('Kokucho', 'Fidalgo Blacky', 'Michael J' and 'Cupid'). A 50-ng sample of genomic DNA was used as a template for qPCR, which was performed with SYBR Premix Ex Taq II (Takara Bio Inc.) or THUNDERBIRD® SYBR qPCR Mix (Toyobo) according to the manufacturer's instructions using the Light Cycler 480 system (Roche Diagnostics K.K.). The qPCR was performed as follows: 95°C for 2 min, followed by 40 cycles at 95°C for 10 s, 55°C for

5 s and 72°C for 20 s. Single-target product amplification was checked using a melting curve. The primers that were used for qPCR are shown in Table S4. To amplify all the alleles, we designed these primers on the identical sequence among multiple alleles (*DvCHS1-1* and *DvCHS1-2* for *DvCHS1*, and *DvCHS2-1*, *MJ-1* and *MJ-2* for *DvCHS2*).

Results

Comparison of pigments in bicolor and red petals

'Yuino' produces not only red-white bicolor petals but also red single-colored petals (Ohno et al. 2016; Fig. 1). The analysis of hydrolysed extracts showed that the red single-colored petals contained anthocyanins (cyanidin and pelargonidin), flavones (apigenin and luteolin) and chalcones (isoliquiritigenin and butein), the composition of which was the same as in the red part of bicolor petals (Fig. 3). The amount of anthocyanins in the red parts of bicolor petals (outside) was nearly the same as in the corresponding part of red single-colored petals, whereas only a small amount of anthocyanins, flavones and chalcones were detected in the white parts (inside) of bicolor petals (Fig. 3). Analysis of the crude extracts showed that the retention time of the peaks of anthocyanins in red single-colored petals and the red part of bicolor petals was the same as in 'Kokucho' petals (data not shown), which mainly accumulate pelargonidin 3-(6"-malonylglucoside)-5-glucoside and cyanidin 3-(6"-malonylglucoside)-5-glucoside (Deguchi et al. 2016). Therefore, it was suggested that the formation of red single-colored petals in 'Yuino' resulted from a loss of the white parts of the petals by recovering flavonoid biosynthesis capacity.

Four chalcone synthase (CHS)-like genes in dahlia

Ohno et al. (2011b) previously demonstrated that the formation of white tips, i.e. the loss of flavonoids from the white parts of petals, results from simultaneous PTGS of two different chalcone synthases, *DvCHS1* and *DvCHS2*. Before analysing the involvement of *CHS* PTGS in the loss of flavonoids in petals and leaves, we first tried to identify all *CHS*-like genes that are expressed in these organs. Two novel *CHS*-like genes were obtained from a database search and transcriptome data, named *DvCHS3* and *DvCHS4*, respectively. For *DvCHS3*, two cDNA sequences were identified from 'Yuino' petals, which were named *DvCHS3-1* and *DvCHS3-2*. The open reading frames of both *DvCHS3-1* and *DvCHS3-2* cDNAs were 1191 bp encoding 397 putative amino acid residues. For *DvCHS4*, one cDNA was detected and its open reading frame was 1170 bp encoding 390 putative amino acid residues. All four *CHS* genes are composed of two exons and one intron, which is typical for the polyketide synthase gene family including *CHS*, and possess a conserved exon-intron junction (Fig. S1).

In the phylogenetic tree based on coding region, *DvCHS1*, *DvCHS2* and *DvCHS4* are close to other *CHS* genes, while *DvCHS3* is close to other polyketide synthases such as stilbene synthase (Fig. 4a). By contrast, in the phylogenetic tree based on putative amino acid sequences, DvCHS1 and DvCHS2 are close to other CHS proteins, while DvCHS3 and DvCHS4 are close to other polyketide synthases (Fig. 4b).

Flavonoid biosynthetic gene expression in petals and leaves

Comparison of the expression levels of flavonoid biosynthetic genes, including four chalcone synthase genes (*DvCHS1*, *DvCHS2*, *DvCHS3* and *DvCHS4*), between red and bicolor petals showed that *DvCHS1* and *DvCHS2* had significantly lower expression levels in the white part of bicolor petals than in red petals, while *DvCHS3*, *DvCHS4* and other flavonoid biosynthetic genes had almost the same expression levels (Fig. 5a).

Western blot analysis also demonstrated that expression levels of CHS protein was lower in the white part of bicolor petals than in red parts (Fig. 5b). By contrast, comparison of the expression levels of flavonoid biosynthetic genes between flavonoid-rich and flavonoid-poor leaves yielded different results, whereby *DvCHS2* but not *DvCHS1* was significantly down-regulated in flavonoid-poor leaves (Fig. 6a). The expression levels of *DvCHS1*, *DvCHS3* and *DvCHS4* were low in both leaf types. This result was confirmed by the RNA-seq analysis. Only two genes were significantly up-regulated while five genes were significantly down-regulated in the flavonoid-rich leaf compared with the flavonoid-poor leaf (Table S5). However, RT-PCR confirmed that six genes were pseudo positive or pseudo negative due to sample bias (data not shown), and so the only gene that was actually differentially expressed between flavonoid-rich and flavonoid-poor leaves was *DvCHS2*. Though the difference of signal intensity between flavonoid-rich leaves and flavonoid-poor leaves was not drastic, Western blot analysis also suggested that expression levels of CHS protein was lower in flavonoid-poor leaves than flavonoid rich leaves (Fig. 6b).

Analysis of small RNAs

Ohno *et al.* (2011b) previously mapped small RNAs from the white part of a bicolor petal onto *DvCHS1* and *DvCHS2* (Fig. 7a). In the current study, we used these data to undertake a mapping analysis of small RNAs for newly isolated *DvCHS3* and *DvCHS4* and recalculated them as matched reads per million reads for comparison. Some small RNAs appeared to be mapped onto *DvCHS4* (Fig. S2, Table 1); however, this sequence was identical to *DvCHS1* and no small RNAs were detected from the *DvCHS4*-specific sequence, suggesting that these small RNAs were derived from *DvCHS1* not *DvCHS4*. Thus, it was demonstrated that *DvCHS3* and *DvCHS4* were not silenced in the white part

of a bicolor petal, presumably due to their low expression. The number of small RNAs matched to each gene is shown in Table 1.

Next, we sequenced small RNAs from a red single-colored petal and performed a mapping analysis for all alleles of *DvCHS1*, *DvCHS2*, *DvCHS3* and *DvCHS4*. The number of total reads of 18–32 nt was 13,681,764 for a red petal, and small RNAs from the red petal were rarely mapped onto any of the four *DvCHS* genes (Fig. 7b; Fig. S2; Table 1). This result suggests that simultaneous PTGS of *DvCHS1* and *DvCHS2* was suppressed in red petals. Small RNAs sharing high identity with some microRNAs (miRNAs) were detected in both small RNA libraries (Table S6).

To determine whether this suppression of *DvCHS2* in flavonoid-poor leaves was post-transcriptional, we first performed an RNA gel blot analysis. Small RNA of *DvCHS2* was detected in flavonoid-poor leaves but not in flavonoid-rich leaves (Fig. 8), which suggested that down-regulation of *DvCHS2* in flavonoid-poor leaves occurs post-transcriptionally. This was confirmed by the small RNA mapping analysis (Fig. 9). While small RNAs from a flavonoid-rich leaf were rarely mapped onto each *CHS* gene (Fig. 9a, Fig. S3, Table 1), 10,625 or 10,872 of 11,465,948 reads were mapped onto *DvCHS2-1* or *DvCHS2-2*, respectively, in a flavonoid-poor leaf (Fig 9b, Table 1). Small RNAs from flavonoid-poor leaf were rarely mapped onto the other *DvCHS* genes (Fig. 9b, Fig. S3, Table 1). Therefore, it was demonstrated that *DvCHS2* genes are silenced post-transcriptionally in flavonoid-poor leaves.

Genomic analysis of DvCHS2

Since all bicolor dahlia cultivars inevitably exhibit petal color lability (i.e. the loss of a white area), it is evident that occurrence of PTGS of *CHS* genes is important for this process. It has previously been reported that specific parts of the genomic sequence are

important for causing endogenous PTGS (Todd and Vodkin 1996; Stam 1997; Kusaba et al. 2003; Della Vedova et al. 2005; Kasai et al. 2007; Tuteja and Vodkin 2008; Morita et al. 2012). Thus, genomic analysis was performed.

The DNA gel blot analysis using *Bam*HI-digested DNA led to one intense bicolor cultivar-specific band being detected when the 3′ or 5′ coding region was used as a probe (Fig. 10a); and when *Hin*dIII-digested DNA was used, one intense bicolor cultivar-specific band was detected when the 3′ coding region was used as a probe (Fig. 10a). The sequence of this band was determined by inverse PCR and identified as the *DvCHS2-1* allele in 'Yuino' (Fig. 10b). Inverse PCR using 'Michael J' genomic DNA identified two other alleles (*MJ-1* and *MJ-2*, respectively), which coincided with the two bands detected in the DNA gel blot analysis of *Hin*dIII using the 3′ probe in 'Michael J'. To confirm these results, genomic PCR was performed using each allele-specific primer. As with the DNA gel blot analysis, the *DvCHS2-1* allele was detected in each of the six tested bicolor cultivars but not in the four tested single-color cultivars (Fig. 10c). The *MJ-1* and *MJ-2* alleles were detected in several cultivars, but there was no correlation between allele retention and flower color (Fig. 10c).

The qPCR analysis for quantifying the genome amount showed that bicolor cultivars had almost the same amount of the *DvCHS1* genomic region but twice as much of the *DvCHS2* genomic region as single-color cultivars (Fig. 11). This applied not only to the gene body, but also to the 3′ flanking region of *DvCHS2*, suggesting that bicolor cultivars retain a duplicated sequence of *DvCHS2*.

Discussion

DvCHS2 *is a functional* CHS *in dahlia*

The *CHS* multigene family contains multiple paralogous *CHS* genes that function in different organs. *CHS*-like genes exhibit different evolutionary patterns, with early or late divergence, and late-diverged *CHS*-like genes have experienced a more rapid non-synonymous substitution rate, yielding new enzyme activities in a relatively short period of time (Han et al. 2014). In the present study, four *CHS*-like genes were isolated from dahlia. A phylogenetic analysis based on the nucleotide sequences suggested that *DvCHS1* and *DvCHS4*, or *DvCHS2* and *DvCHS3* originated from the same gene (Fig. 4a). By contrast, a phylogenetic analysis based on putative amino acid sequences showed that DvCHS3 and DvCHS4 were more closely related to Gh2PS or VvSTS1 than other CHS genes (Fig. 4b), suggesting that these genes diverged from the other *CHS* genes more recently but now exhibit other enzymatic activities.

In gerbera (*Gerbera hybrida*), *GhCHS1*, which is orthologous to *DvCHS2*, is associated with flavonoid biosynthesis in petals, while *GhCHS4*, which is orthologous to *DvCHS1*, is associated with vegetative tissues (Helariutta et al. 1995, Deng et al. 2014). However, in dahlia, *DvCHS2* is expressed in both petals and leaves, and its expression completely coincides with flavonoid biosynthesis, i.e. the loss of expression of *DvCHS2* in petals results in the loss of anthocyanin, flavone and butein synthesis (Ohno et al. 2011b; Fig. 3), and the loss of expression of *DvCHS2* in leaves results in the loss of flavonol and butein synthesis (Ohno et al. 2016, 2017). Therefore, it appears that the DvCHS2 protein may be the functional CHS enzyme in both petals and leaves, and so is associated with all flavonoid biosynthesis in dahlia. *DvCHS1* is under the regulation of the basic helix-loop-helix transcription factor DvIVS (Ohno et al. 2011a) and retains the preserved sequences of *CHS* genes (Ohno et al. 2011b), suggesting that it also has CHS activity in dahlia.

476 *Phenotypic lability in 'Yuino' is associated with the occurrence of* DvCHS2 *PTGS*

477 'Yuino' produces red single-colored petals in addition to original red-white bicolor petals
478 (Fig. 1; Ohno et al. 2016). Almost no flavonoids were detected in the white parts of petals
479 (Fig. 3) due to PTGS of both *DvCHS1* and *DvCHS2* (Ohno et al. 2011b). However, red-
480 colored petals accumulated flavonoids (Fig. 3), suggesting that PTGS of *CHS* was
481 suppressed in these. In fact, expression levels of *DvCHS1* and *DvCHS2* are higher in the
482 inner area of red petal than the corresponding pure white area of bicolor petals (Fig. 5a).
483 Western blot analysis also suggested that CHS protein expression was recovered in the
484 inner area of red petal (Fig. 5b). In red petals, small RNAs of *DvCHS2* were rarely
485 detected by RNA gel blot analysis (Fig. 8) and almost no small RNAs were mapped on
486 *DvCHS* genes (Fig. 7b) suggesting PTGS of *CHS* was suppressed in red petals.

487 Ohno et al. (2016) previously detected a strong relationship between
488 inflorescence color and leaf phenotype, whereby red petal-producing plants accumulated
489 flavonoids in their leaves while plants without flavonoids in their leaves produced only
490 bicolor petals. This suggests that the formation of the white part of a petal is related to the
491 flavonoid biosynthetic potential of the shoot. The flavonoids in leaves have been
492 identified as butein and flavonol derivatives by nuclear magnetic resonance analysis
493 (Ohno et al. 2017). In the present study, only *DvCHS2* had lower expression in flavonoid-
494 poor leaves than in flavonoid-rich leaves, whereas other flavonoid biosynthetic genes had
495 almost the same expression levels (Fig. 6a). The small RNAs of a flavonoid-poor leaf
496 were detected by RNA gel blot analysis (Fig. 8) and mapped onto the *DvCHS2* gene (Fig.
497 9b, Table 1), indicating that this suppression of *DvCHS2* occurs post-transcriptionally.
498 Therefore, PTGS of *DvCHS2* is associated with the absence of leaf flavonoid
499 accumulation, indicating that PTGS of *CHS* in both petals and leaves is tightly linked to
500 petal color lability.

This then leads to the new question of why PTGS of *CHS* is not occurred in red petals and flavonoid-rich leaves. There are two possible explanations for this: *CHS*-specific PTGS has ceased or PTGS of all genes has ceased. The small RNAs sharing high identity with miR159 or miR165 or unknown small RNAs were detected in both red-colored petals and the white part of bicolor petals (Table S6), suggesting that general PTGS pathway was functional in both petal types. Therefore, it could be that *CHS*-specific PTGS has ceased in red petals. A similar trend was also observed in leaves. It was notable that although seven genes were differentially expressed between a flavonoid-rich and a flavonoid-poor leaf by RNA-seq analysis (Table S5), only *DvCHS2* was substantially different (Table S5), whereas the other genes were pseudo positive. This suggests that the suppression of PTGS in flavonoid-rich leaves is also *DvCHS2*-specific, but not the PTGS component itself.

In the case of soybean (*Glycine max*), it has been shown that the silencing of *CHS* gene family members occurs only in the seed coats and not in other organs (Tuteja et al. 2004, 2009), and that both primary and secondary *CHS* siRNAs are not significantly produced in the germinated cotyledon, immature cotyledon, leaf, root, shoot tip or stem tissues (Cho et al. 2013). However, in bicolor dahlia ‘Yuino’, the production of *CHS* siRNAs was not limited to the petal tips but also observed in the leaves. This *CHS* siRNA-producing state was assumed to be maintained after vegetative propagation because plants that are propagated from flavonoid-poor plants, in which *CHS* PTGS occurs, produce only bicolor petals (Ohno et al. 2016).

Genomic background for PTGS of CHS *genes*

In dahlia, two different *CHS* genes were silenced in the white part of bicolor petals: *DvCHS1* and *DvCHS2*. *CHS* siRNA was also detected in the pure white part of the yellow-

white bicolor cultivar 'OriW1', which does not express *DvCHS1* in the petals, suggesting that the PTGS of *DvCHS2* can be induced without *DvCHS1* expression (Ohno et al. 2011b). Thus, it had been presumed that *DvCHS2* was a potential causal gene of *CHS* PTGS in bicolor dahlia and that the silencing of *DvCHS1* was incidental due to high homology with some secondary *DvCHS2* siRNAs. This was supported by our analysis of the leaves, in which only *DvCHS2* was silenced because *DvCHS1* is expressed at a relatively low level in both flavonoid-rich and flavonoid-poor leaves (Figs. 6a, 9).

It has previously been reported that specific parts of the genomic sequence, such as inverted repeats, cause endogenous PTGS (Todd and Vodkin 1996; Stam 1997; Kusaba et al. 2003; Della Vedova et al. 2005; Kasai et al. 2007; Tuteja and Vodkin 2008; Morita et al. 2012). With respect to PTGS of *CHS*, inverted repeats of *CHS* are a potent cause in maize (*Zea mays*; Della Vedova et al. 2005) and soybean (Todd and Vodkin 1996; Kasai et al. 2007; Tuteja and Vodkin 2008), while a tandem repeat is a potent cause in petunia (*Petunia hybrida*; Stam 1997; Morita et al. 2012). DNA gel blot analysis suggested the existence of a bicolor cultivar-specific *DvCHS2* allele, which is identical to 'Yuino' *DvCHS2-1* (Fig. 10a, b). This allele was only detected in bicolor cultivars (Fig. 10c), suggesting that it is linked to the silencing causal gene.

Quantification of the genome amount showed that bicolor cultivars contain twice as much of the *DvCHS2* region but almost the same amount of the *DvCHS1* region as single-color cultivars (Fig. 11). This suggests that bicolor cultivars have a duplicated *DvCHS2* region. The 3′ proximal *DvCHS2* region also doubled in bicolor cultivars (Fig. 11), whereas no repeat sequence of *CHS* was detected from 3-kb downstream of *DvCHS2-1* (Fig. 10b). The DNA gel blot analysis digested with *Bam*HI detected intense bands of approximately 8 kb with the 5′ probe and 10 kb with the 3′ probe (Fig. 10a), suggesting that at least an 18-kb region that includes *DvCHS2* is duplicated in bicolor cultivars. This

551 region is a strong candidate for the *CHS* PTGS causal gene, but further analysis is required
552 to confirm this.
553
554 *Candidate mechanism for petal color lability in bicolor dahlias*
555 The causal gene of PTGS of *DvCHS* is presumed to be *DvCHS2* (see above), and so petal
556 color lability in bicolor dahlias could be interpreted as resulting from the switching on
557 and off of *DvCHS2* PTGS. Since all shoot organs including petals and leaves are
558 differentiated from the shoot apical meristem (SAM), this switching could occur in the
559 SAM. Consequently, here we propose a candidate model of SAM state for each flower
560 color pattern. This model is based on the observation that when both red petals and bicolor
561 petals occur in the same inflorescence, red petals were located inevitably in the outer
562 whorls rather than bicolor petals, and the inverse pattern was never observed (Ohno et al.,
563 2016). This indicates an obvious direction for the SAM state from red petal to bicolor
564 petal. Considering the strong link between petal color and leaf flavonoid accumulation
565 (Ohno et al. 2016), the SAM state of single-colored petal formation and flavonoid-rich
566 leaves could be defined as a 'switch OFF' of *DvCHS2* PTGS, while the SAM state of
567 bicolor petal formation and flavonoid-poor leaves is a 'switch ON' of *DvCHS2* PTGS.
568 Therefore, when the SAM maintains a 'switch OFF' state, the inflorescence will be a
569 single color due to the absence of *DvCHS2* PTGS, whereas when SAM maintains a
570 'switch ON' state, the inflorescence will be bicolor as a result of *DvCHS2* PTGS.
571 Furthermore, if the SAM maintains a 'switch ON' state sectorally, the inflorescence will
572 be mixed with sectorial single-colored petals; and if the switch of *CHS* PTGS turns 'ON'
573 after the formation of outer whorl petals, the inflorescence will be mixed with single-
574 colored petals in the outer whorls. Original bicolor cultivars may change to 'switch ON'
575 before formation of the inflorescence. The timing of switching depends on the plant,

because plants that produce flavonoid-rich leaves could bloom both bicolor and red inflorescences (Ohno et al. 2016). In this case, it is assumed that if switching occurs before flowering, the inflorescence will be bicolor, whereas if switching does not occur, the inflorescence will be red.

The above model can explain the phenotypic relationship between petal color and leaf flavonoid accumulation. However, another factor is required to explain the lability itself. The phenomenon of color lability is not limited to dahlias, but is also found in other plants, such as *Rhododendron* spp. and transgenic petunia, suggesting that there may be a common mechanism across species. Transgenic petunia plants carrying a sense *CHS* transgene (Jorgensen 1995) or antisense *CHS* transgene (van der Krol et al. 1990) also exhibit flower color lability. In co-suppressed petunia carrying a sense *CHS* transgene, the expression of *CHS* is suppressed in the leaf tissues of white branches and reverted in the leaf tissues of the revertant violet branches (Napoli et al. 1990). In this phenotypic reversion, it was demonstrated that epigenetic changes that interfere with the initiation of transgene transcription lead to a reversion of the PTGS phenotype (Kanazawa et al. 2007). Therefore, an endogenous factor is inferred to be involved in this switch control, perhaps an epigenetic factor such as DNA methylation. When the gene or locus that triggers *DvCHS* PTGS is activated in the SAM, an endogenous factor might fully or sectorally suppress its activation in the SAM, resulting in petal color lability. Recently, it was reported that soybean Argonaute5 (AGO5) affects the distribution of siRNAs targeting the *CHS* genes in the seed coat (Cho et al. 2017). In nonfunctional AGO5 background (*k1*), production of *CHS* siRNAs was suppressed even in the presence of the normally dominant *I* allele. Thus, not only *CHS* itself but also AGO and other components of RNA-induced silencing complex is a candidate trigger gene of *CHS* PTGS. Isolation of the gene or locus that triggers *DvCHS* PTGS would be of great value in further elucidating the

mechanism behind color lability.

Acknowledgements

We thank for Dr. Nakayama and Dr. Waki (Tohoku University, Japan) for kindly supplying Anti-GmCHS7 peptide antibody, and for Soo-Jung Yang for supporting RNA-seq analysis.

Funding: This study was supported by Grants-in Aid for Japan Society for the Promotion of Science (JSPS) Fellows (No. 12J03517) and Grant-in-Aid for Young Scientists (B) (No. 15K18638) from the JSPS to S. O.

Conflict of Interest: The authors declare that they have no conflict of interest.

Supplemental materials

Table S1. Primers used for the isolation of *DvCHS3* and *DvCHS4*.

Table S2. Primers used for real-time RT-PCR.

Table S3. Primers used for identification of the *DvCHS2* flanking region.

Table S4. Primers used for qPCR for genomic quantification.

Table S5. Genes that showed significantly different expression levels between a

626 flavonoid-rich leaf and a flavonoid-poor leaf in *Dahlia variabilis* ‘Yuino’.

627 **Table S6.** Top 80 most highly abundant small RNAs for which the number of total reads
628 per million (RPM) was over 1000 in a red petal and the white part of a bicolor petal of
629 *Dahlia variabilis* ‘Yuino’.

630 **Fig. S1.** Genome structure of *DvCHS1–DvCHS4*.

631 **Fig. S2.** Mapping of chalcone synthase (*CHS*) small RNAs from petals onto *DvCHS3* and
632 *DvCHS4*.

633 **Fig. S3.** Mapping of chalcone synthase (*CHS*) small RNAs from leaves onto *DvCHS3*
634 and *DvCHS4*.

635
636
637
638
639
640
641
642
643
644
645
646
647
648
649
650

651 **Figure legends**

652

653 **Fig. 1.** Petal color lability in field-grown *Dahlia variabilis* 'Yuino'. Both bicolor petals
654 and red petals were produced in the inflorescence on the right.

655

656 **Fig. 2.** Flavonoid biosynthetic pathway in dahlia (*Dahlia variabilis*). This figure was
657 based on Ohno et al. (2011a) with some modifications. ANS, anthocyanidin synthase;
658 CH3H, chalcone 3-hydroxylase; CHI, chalcone isomerase; CHR, chalcone reductase;
659 CHS, chalcone synthase; DFR, dihydroflavonol 4-reductase; F3H, flavanone 3-
660 hydroxylase; F3′H, flavonoid 3′-hydroxylase; FLS, flavonol synthase; FNS, flavone
661 synthase; GST, glutathione S-transferase; GT, anthocyanidin glucosyltransferase; 3MaT,
662 anthocyanidin 3-*O*-glucoside-6″-*O*-malonyltransferase.

663

664 **Fig. 3.** Amount of flavonoid per 100 mg fresh weight (FW) of red and bicolor petals of
665 *Dahlia variabilis* 'Yuino'. Bicolor petals were separated into the outside red area (Bicolor
666 out) and the inner white area (Bicolor in) and collected separately. Red petals were also
667 separated in the same way as bicolor petals, namely separated into the outside area (Red
668 out) and the inner area (Red in). All data represent the mean ± SE (n = 6). Cy, cyanidin;
669 Pg, pelargonidin; Lt, luteolin; Ap, apigenin; Iso, isoliquiritigenin; Bt, butein.

670

671 **Fig. 4.** Phylogenetic tree for chalcone synthase (CHS). a, Phylogenetic tree based on the
672 coding regions; b, phylogenetic tree based on putative amino acid sequences. The
673 bootstrap values of 1,000 retrials are indicated on each branch and the bar indicates a
674 genetic distance of 0.1. The abbreviation in front of each coding region/protein indicates
675 the plant species: Am, *Antirrhinum majus*; At, *Arabidopsis thaliana*; Dv, *Dahlia*

676 *variabilis*; Gh, *Gerbera hybrida*; Gm, *Glycine max*; In, *Ipomoea nil*; Ms, *Medicago*
677 *sativa*; Ph, *Petunia hybrida*; Vv, *Vitis vinifera*; Zm, *Zea mays*. Proteins are abbreviated as
678 follows: STS, stilbene synthase; 2PS, 2-pyrone synthase.
679
680 **Fig. 5.** Expression analysis of flavonoid biosynthetic pathway in petals. Bicolor petals
681 were separated into the outside red area (Bicolor out) and the inner white area (Bicolor
682 in) and collected separately. Red petals were also separated in the same way as bicolor
683 petals, namely separated into the outside area (Red out) and the inner area (Red in). a,
684 Relative expression levels of flavonoid biosynthetic genes and transcription factors in red
685 and bicolor petals of *Dahlia variabilis* 'Yuino' by real-time RT-PCR. All data represent
686 the mean ± SE (n = 3). Each value represents the expression level relative to that of inside
687 part of red petal (Red in). *DvActin* was used as the internal standard. n.d., not detected. b,
688 Western blot analysis of CHS in petals. P. C. (positive control): recombinant DvCHS2-
689 6xHN-C. Two biological replications were performed for each part.
690
691 **Fig. 6.** Expression analysis of flavonoid biosynthetic pathway in flavonoid-rich and
692 flavonoid-poor leaves. a, Relative expression levels of flavonoid biosynthetic gene in
693 leaves of *Dahlia variabilis* 'Yuino' by real-time RT-PCR. Scores were calculated relative
694 to flavonoid-poor leaves (= 1). The vertical bars indicate the SE (n = 6). b, Western blot
695 analysis of CHS protein in leaves. P. C. (positive control): recombinant DvCHS2-6xHN-
696 C. Three biological replications were performed for each flavonoid-rich leaf and
697 flavonoid-poor leaf.
698
699 **Fig. 7.** Mapping of chalcone synthase (*CHS*) small RNAs from petals onto *DvCHS1* and
700 *DvCHS2*. a, white part of a bicolor petal. b, a red petal; Small RNAs of 18–32 nt with a

100% match to *DvCHS1-1*, *DvCHS1-2*, *DvCHS2-1*or *DvCHS2-2* were mapped onto either the sense (above the *x*-axis) or antisense (below the *x*-axis) strand. The number of total reads of 18–32 nt was 17,455,041 for the white part of a bicolor petal and 13,681,764 for a red petal. To compare the white area of a bicolor petal with a red petal, values for *DvCHS1-1*, *DvCHS1-2*, *DvCHS2-1* and *DvCHS2-2* in the white part of a bicolor petal were obtained from Ohno *et al.* (2011b) and recalculated as the number of matched reads per million reads.

Fig. 8. Detection of chalcone synthase (*CHS*) small RNAs in *Dahlia variabilis* 'Yuino' leaves by RNA gel blot analysis. Three biological replications were performed for each flavonoid-rich leaf and flavonoid-poor leaf. Whole part of bicolor petals were used as a positive control.

Fig. 9. Mapping of chalcone synthase (*CHS*) small RNAs from leaves onto *DvCHS1* and *DvCHS2*. a, a flavonoid-rich leaf; b, a flavonoid-poor leaf. Small RNAs of 18–30 nt with a 100% match to *DvCHS1-1*, *DvCHS1-2*, *DvCHS2-1* or *DvCHS2-2* were mapped onto either the sense (above the *x*-axis) or antisense (below the *x*-axis) strand. The number of total reads of 18–30 nt was 12,046,092 for a flavonoid-rich leaf and 11,465,948 for a flavonoid-poor leaf.

Fig. 10. Genomic structure of *DvCHS2*. a, DNA gel blot analysis of *DvCHS2*; the blot was hybridised with a 5′ probe (left two panels) and a 3′ probe (right two panels). b, Location of primers, probes and restriction enzyme recognition sites of *DvCHS2* alleles; B and H indicate restriction enzyme recognition sites of *Bam*HI and *Hin*dIII; arrows indicate the position of the primers used in c. c, genomic polymerase chain reaction (PCR)

726 analysis of allele-specific sequences in the 3′ flanking region of *DvCHS2*. Numbers above
727 the lanes indicate each cultivar: 1, ‘Yuino’; 2, ‘Matsuribayashi’; 3, ‘Kazusa-shiranami’;
728 4, ‘Santa Claus’; 5, ‘OriW1’; 6, ‘OriW2’; 7, ‘Kokucho’; 8, ‘Ms. Noir’; 9, ‘Yukino’ and
729 10, ‘Michael J’.
730
731 **Fig. 11.** Quantification of the *DvCHS1* and *DvCHS2* genomic regions. ①-⑤ indicates
732 position of designed primers. Primers were designed on the identical sequence among
733 multiple alleles (*DvCHS1-1* and *DvCHS1-2* for *DvCHS1*, and *DvCHS2-1*, *MJ-1* and *MJ-*
734 *2* for *DvCHS2*). qPCR analyses to quantify the amount of the genomic regions of *DvCHS1*
735 and *DvCHS2*. Data represent the mean ± SD scores of three technical replicates of three
736 biological replicates relative to ‘Yuino’ (= 1).
737
738
739
740
741
742
743
744
745
746
747
748
749
750

References

Cho YB, Jones SI, Vodkin L (2013) The transition from primary siRNAs to amplified secondary siRNAs that regulate chalcone synthase during development of *Glycine max* seed coats. PLoS ONE 8: e76954.

Cho YB, Jones SI, Vodkin LO (2017) Mutations in *Argonaute5* illuminate epistatic interactions of the *K1* and *I* loci leading to saddle seed color patterns in *Glycine max*. Plant Cell 29: 708-725.

Deguchi A, Ohno S, Hosokawa M, Tatsuzawa F, Doi M (2013) Endogenous post-transcriptional gene silencing of flavone synthase resulting in high accumulation of anthocyanins in black dahlia cultivars. Planta 237:1325-1335.

Deguchi A, Tatsuzawa F, Hosokawa M, Doi M, Ohno S (2016) Quantitative evaluation of the contribution of four major anthocyanins to black flower coloring of dahlia petals. Hort J 85:340-350.

Della Vedova CB, Lorbiecke R, Kirsch H, Schulte MB, Scheets K, Borchert LM, Scheffler BE, Wienand U, Cone KC, Birchler JA (2005) The dominant inhibitory chalcone synthase allele *C2-Idf* (inhibitor diffuse) from *Zea mays* (L.) acts via an endogenous RNA silencing mechanism. Genetics 170:1989-2002.

Deng X, Bashandy H, Ainasoja M, Kontturi J, Pietiäinen M, Laitinen RAE, Albert VA, Valkonen JPT, Elomaa P, Teeri TH (2014) Functional diversification of duplicated

776 chalcone synthase genes in anthocyanin biosynthesis of *Gerbera hybrida*. New Phytol
777 201:1469-1483.
778
779 Gatt M, Ding H, Hammett K, Murray B (1998) Polyploidy and evolution in wild and
780 cultivated Dahlia species. Ann Bot 81:647-656.
781
782 Han Y, Zhao W, Wang Z, Zhu J, Liu Q (2014) Molecular evolution and sequence
783 divergence of plant chalcone synthase and chalcone synthase-Like genes. Genetica
784 142:215-225.
785
786 Helariutta Y, Elomaa P, Kotilainen M, Griesbach RJ, Schroder J, Teeri TH (1995)
787 Chalcone synthase-like genes active during corolla development are differentially
788 expressed and encode enzymes with different catalytic properties in *Gerbera hybrida*
789 (Asteraceae). Plant Mol Biol 28:47-60.
790
791 Hodgins KA, Lai Z, Oliveira LO, Still DW, Scascitelli M, Barker MS, Kane NC,
792 Dempewolf H, Kozik A, Kesseli RV, Burke JM, Michelmore RW, Rieseberg LH (2014)
793 Genomics of compositae crops: Reference transcriptome assemblies and evidence of
794 hybridization with wild relatives. Mol Ecol Resources 14:166-177.
795
796 Jorgensen RA (1995) Cosuppression, flower color patterns, and metastable gene
797 expression states. Science 268:686-691.
798
799 Kanazawa A, O'Dell M, Hellens RP (2007) Epigenetic inactivation of chalcone synthase-
800 A transgene transcription in petunia leads to a reversion of the post-transcriptional gene

801 silencing phenotype. Plant Cell Physiol 48:638-647.

802

803 Kasai A, Kasai K, Yumoto S, Senda M (2007) Structural features of *GmIRCHS*, candidate
804 of the *I* gene inhibiting seed coat pigmentation in soybean: Implications for inducing
805 endogenous RNA silencing of chalcone synthase genes. Plant Mol Biol 64:467-479.

806

807 Konishi, K. and K. Inaba (1964) Studies on flowering control of dahlia. I. On optimum
808 day-length. J. Japan. Soc. Hort. Sci. 33: 171-180 (In Japanese with English abstract).

809

810 Kusaba M, Miyahara K, Iida S, Fukuoka H, Takano T, Sassa H, Nishimura M, Nishio T
811 (2003) Low glutelin content1: A dominant mutation that suppresses the glutelin
812 multigene family via RNA silencing in rice. Plant Cell 15:1455-1467.

813

814 Lawrence WJC (1931) Mutation or segregation in the octoploid *Dahlia variabilis*. J Genet
815 24: 307-324.

816

817 Morita Y, Saito R, Ban Y, Tanikawa N, Kuchitsu K, Ando T, Yoshikawa M, Habu Y,
818 Ozeki Y, Nakayama M (2012) Tandemly arranged *chalcone synthase A* genes contribute
819 to the spatially regulated expression of siRNA and the natural bicolor floral phenotype in
820 *Petunia hybrida*. Plant J 70:739-749.

821

822 Napoli C, Lemieux C, Jorgensen R (1990) Introduction of a chimeric chalcone synthase
823 gene into petunia results in reversible co-suppression of homologous genes in trans. Plant
824 Cell 2:279-289.

825

826 Ohno S, Deguchi A, Hosokawa M, Tatsuzawa F, Doi M (2013) A basic helix-loop-helix
827 transcription factor DvIVS determines flower color intensity in cyanic dahlia cultivars.
828 Planta 238:331-343.
829
830 Ohno S, Hori W, Hosokawa M, Tatsuzawa F, Doi M (2016) Petal color is associated with
831 leaf flavonoid accumulation in a labile bicolor flowering dahlia (*Dahlia variabilis*)
832 'Yuino'. Hort J 85:177-186.
833
834 Ohno S, Hori W, Hosokawa M, Tatsuzawa F, Doi M. (2017). Identification of flavonoids
835 in leaves of a labile bicolor flowering dahlia (*Dahlia variabilis*) 'Yuino'. Hort J: In press.
836 doi: 10.2503/hortj.OKD-099.
837
838 Ohno S, Hosokawa M, Hoshino A, Kitamura Y, Morita Y, Park K, Nakashima A, Deguchi
839 A, Tatsuzawa F, Doi M, Iida S, Yazawa S (2011a) A bHLH transcription factor, *DvIVS*, is
840 involved in regulation of anthocyanin synthesis in dahlia (*Dahlia variabilis*). J Exp Bot
841 62:5105-5116.
842
843 Ohno S, Hosokawa M, Kojima M, Kitamura Y, Hoshino A, Tatsuzawa F, Doi M, Yazawa
844 S (2011b) Simultaneous post-transcriptional gene silencing of two different chalcone
845 synthase genes resulting in pure white flowers in the octoploid dahlia. Planta 234:945-
846 958.
847
848 Robinson MD, McCarthy DJ, Smyth GK (2010) edgeR: A Bioconductor package for
849 differential expression analysis of digital gene expression data. Bioinformatics 26:139-
850 140.

Saitou N, Nei M (1987) The neighbor-joining method: a new method for reconstructing phylogenetic trees. Mol Biol Evol 4:406-425.

Stam, M (1997) Post-transcriptional silencing of flower pigmentation genes in *Petunia hybrida* by (trans)gene repeats. PhD thesis, Vrije Universiteit.

Tammes T, Groeneveld-Huisman AF (1939) Local pigment suppression in the flowers of *Dahlia variabilis* Desf. Genetica 21:301-324.

Temsch EM, Greilhuber J, Hammett KRW, Murray BG (2008) Genome size in *Dahlia* Cav. (Asteraceae-Coreopsideae). Plant Sys Evol 276:157-166.

Todd JJ, Vodkin LO (1996) Duplications that suppress and deletions that restore expression from a CHS multigene family. Plant Cell 8: 687-699.

Tuteja JH, Vodkin LO (2008) Structural features of the endogenous *CHS* silencing and target loci in the soybean genome. Plant Genome 48: 49-69.

Tuteja JH, Clough SJ, Chan W-, Vodkin LO (2004) Tissue-specific gene silencing mediated by a naturally occurring chalcone synthase gene cluster in *Glycine max*. Plant Cell 16:819-835.

874 Tuteja JH, Zabala G, Varala K, Hudson M, Vodkin LO (2009) Endogenous, tissue-
875 specific short interfering RNAs silence the chalcone synthase gene family in *Glycine max*
876 seed coats. Plant Cell 21:3063-3077.
877
878 van der Krol AR, Mur LA, de Lange P, Gerats AGM, Mol JNM, Stuitje AR (1990)
879 Antisense chalcone synthase genes in petunia: Visualization of variable transgene
880 expression. Mol Gen Genet 220:204-212.
881
882 Wang W, Tang K, Yang HR, Wen PF, Zhang P, Wang HL, Huang WD (2010) Distribution
883 of resveratrol and stilbene synthase in young grape plants (*Vitis vinifera* L. cv. Cabernet
884 Sauvignon) and the effect of UV-C on its accumulation. Plant Phisiol Biochem 48: 142-
885 152.
886
887
888
889
890
891
892
893
894
895
896
897
898

899 **Table**

900

Table 1. The number of small RNAs matched to each chalcone synthase (*CHS*) gene.

		Petal		Leaf	
		Red petal	White part of bicolor petal	Flavonoid-rich leaf	Flavonoid-poor leaf
Total Read		13,681,764	17,455,041	12,046,092	11,465,948
Gene	*CHS1-1*	665	63,361	1	7
	CHS1-2	656	61,594	2	2
	CHS2-1	483	371,899	83	10,625
	CHS2-2	337	296,406	36	10,872
	CHS3-1	1	2	0	1
	CHS3-2	1	0	0	0
	CHS4	11	148	0	0

901

902

903 **Figures**

904

905 **Fig. 1**

906

907

908

909 **Fig. 2**

910

911

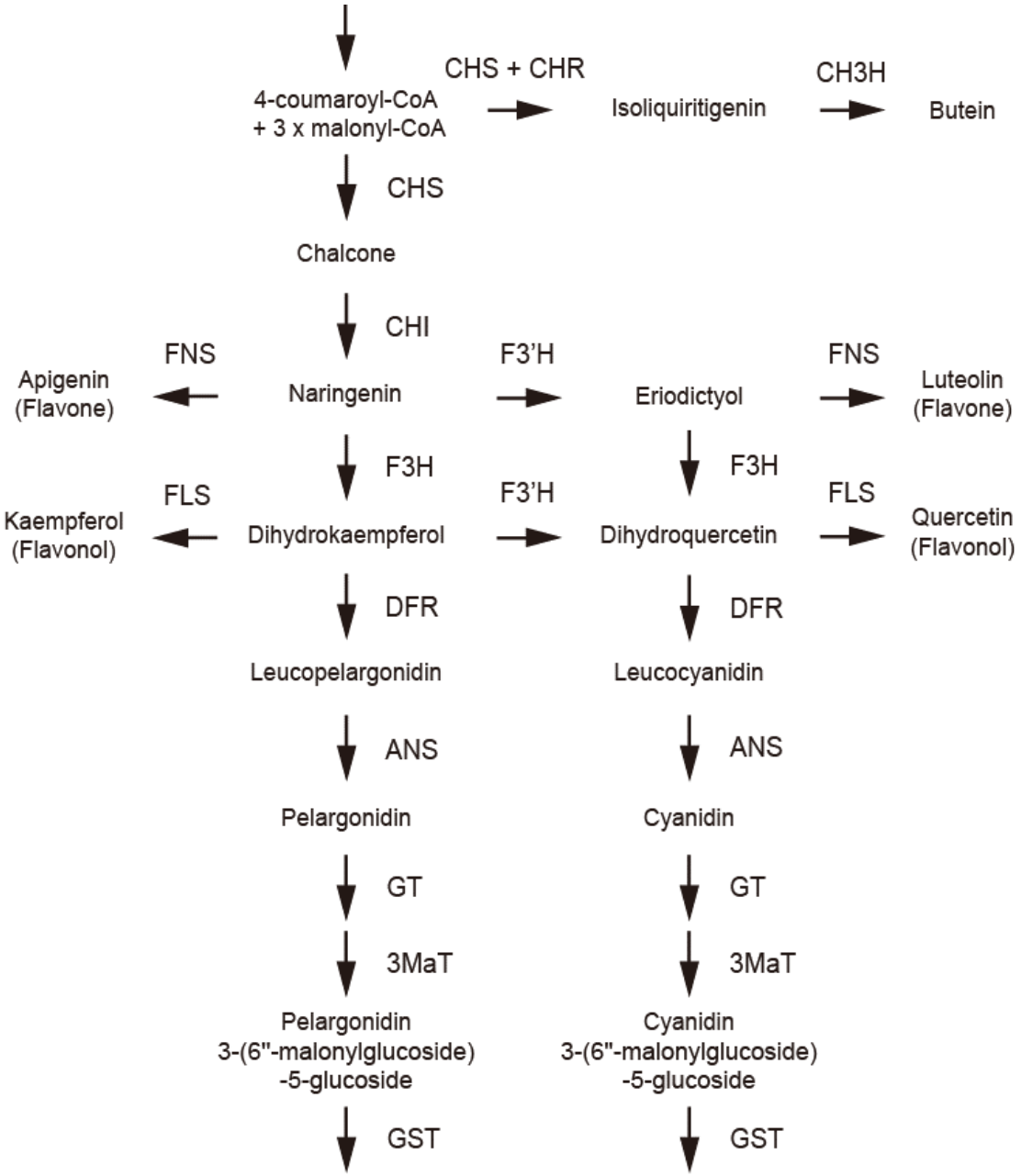

912

913

914 **Fig. 3**

915

916

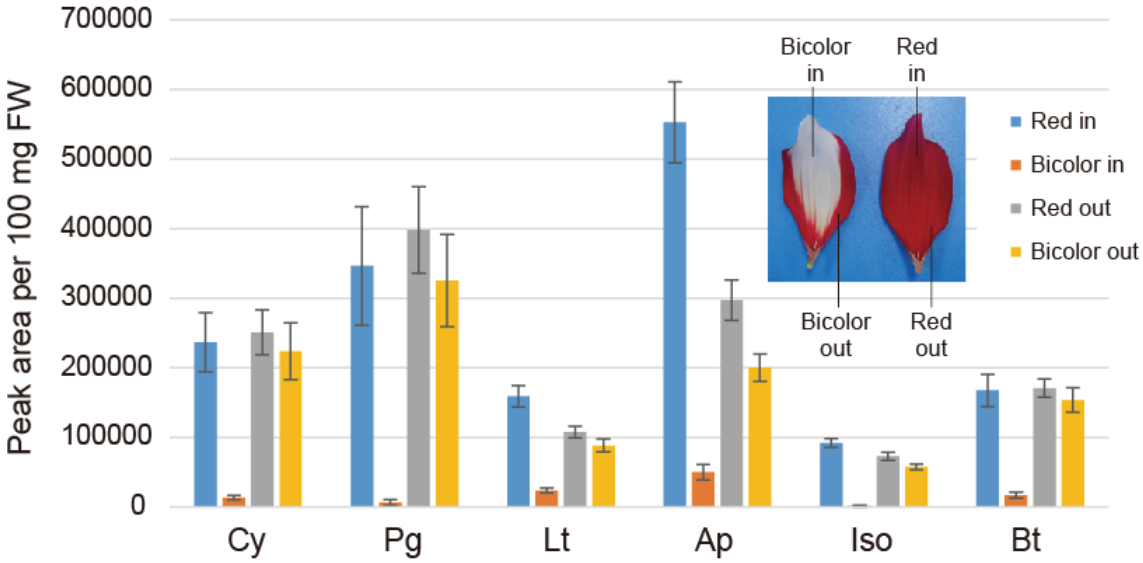

917

918

919

920 **Fig. 4**

921

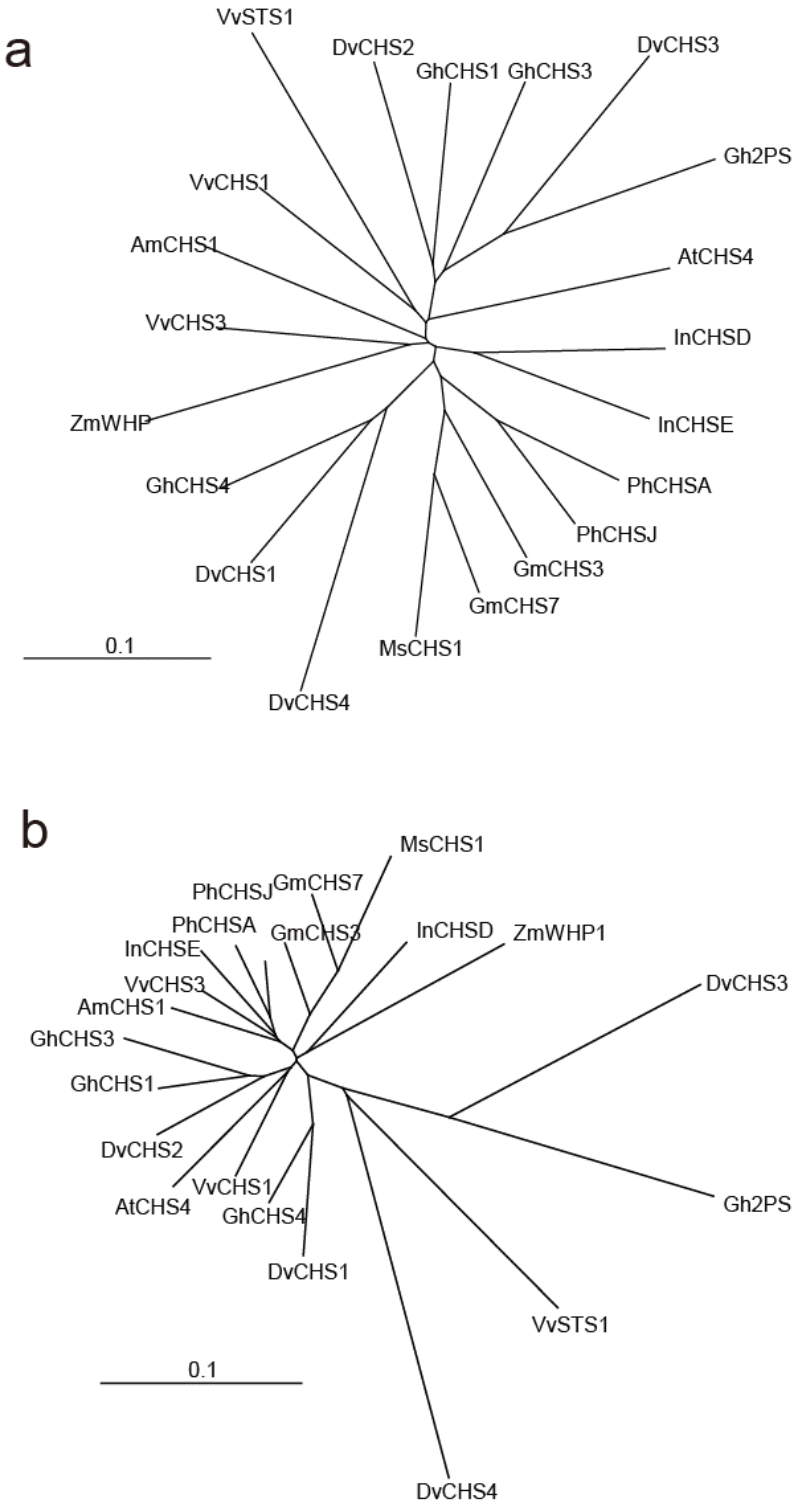

922

923

924 **Fig. 5**

925

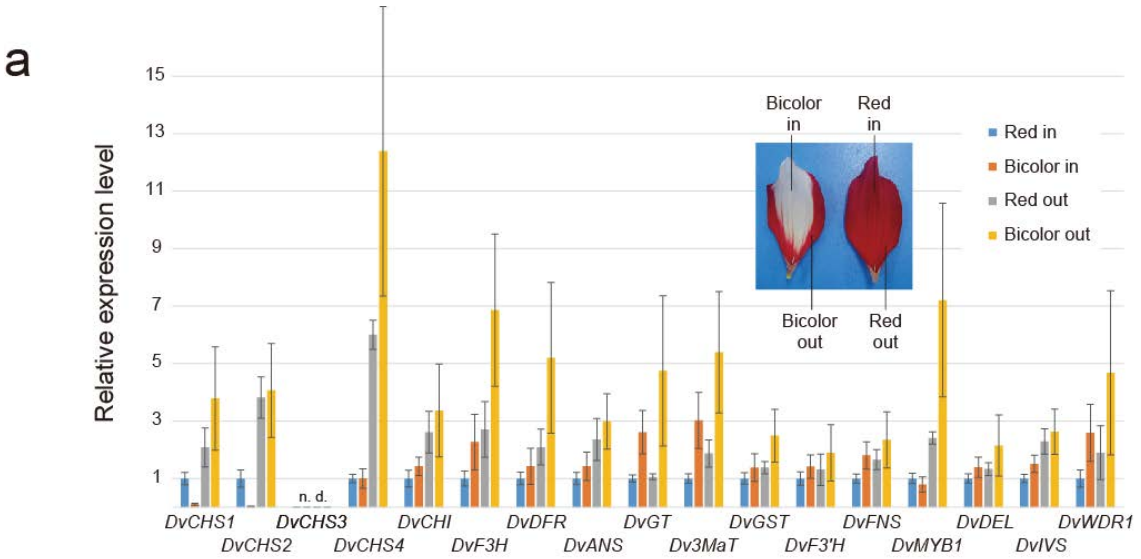

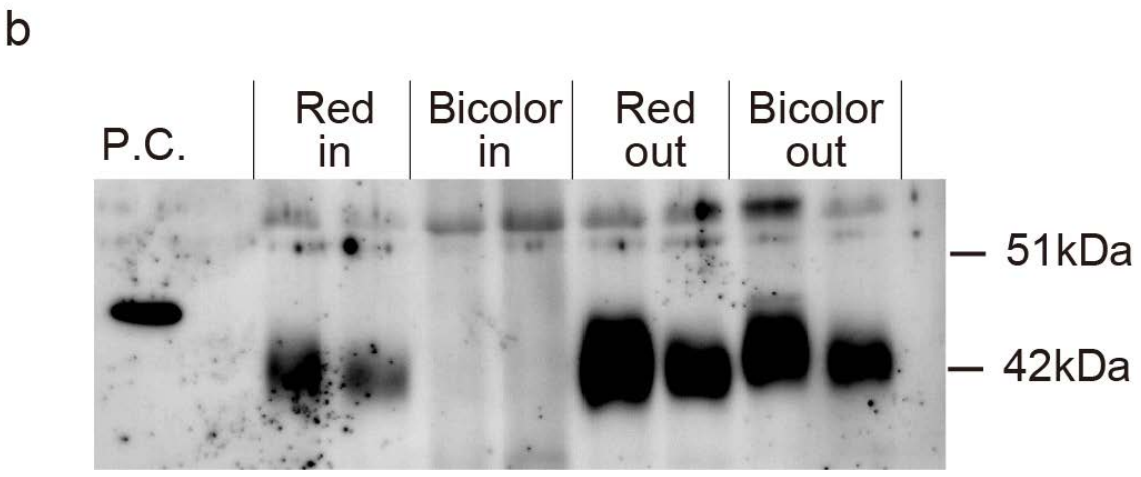

926

927

928 **Fig. 6**

929

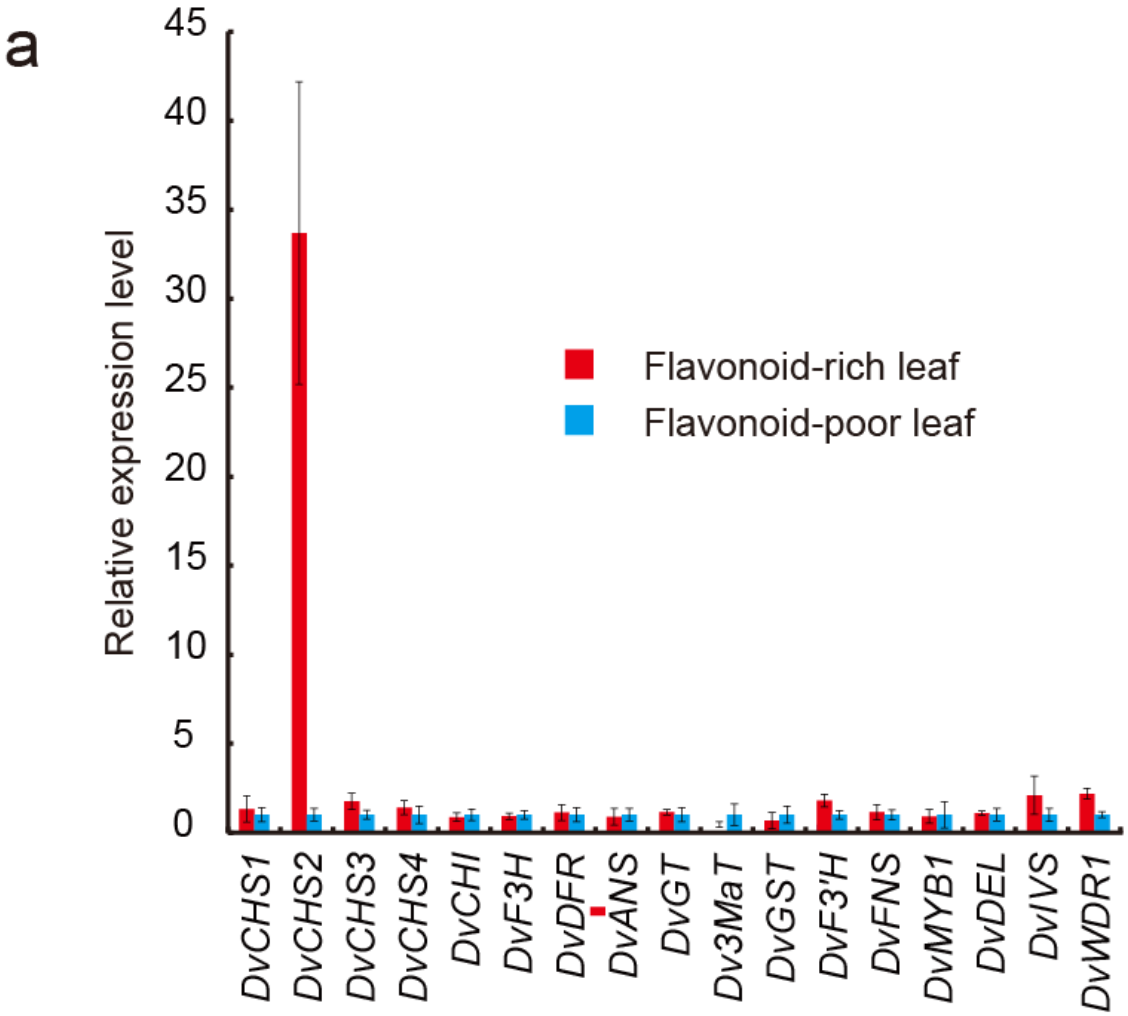

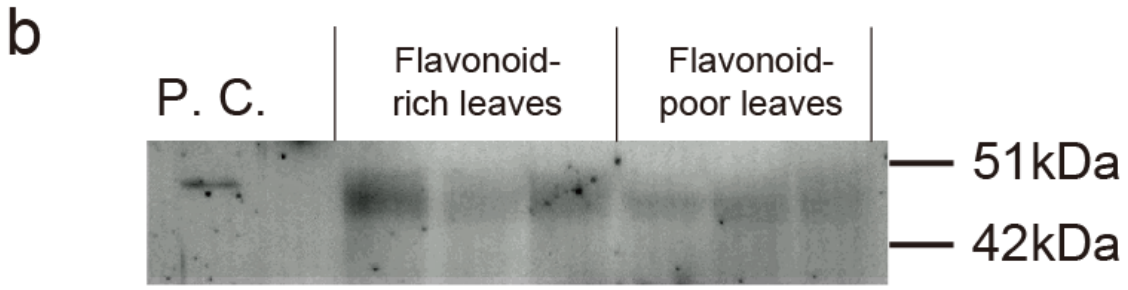

930

931

932

933 **Fig. 7**

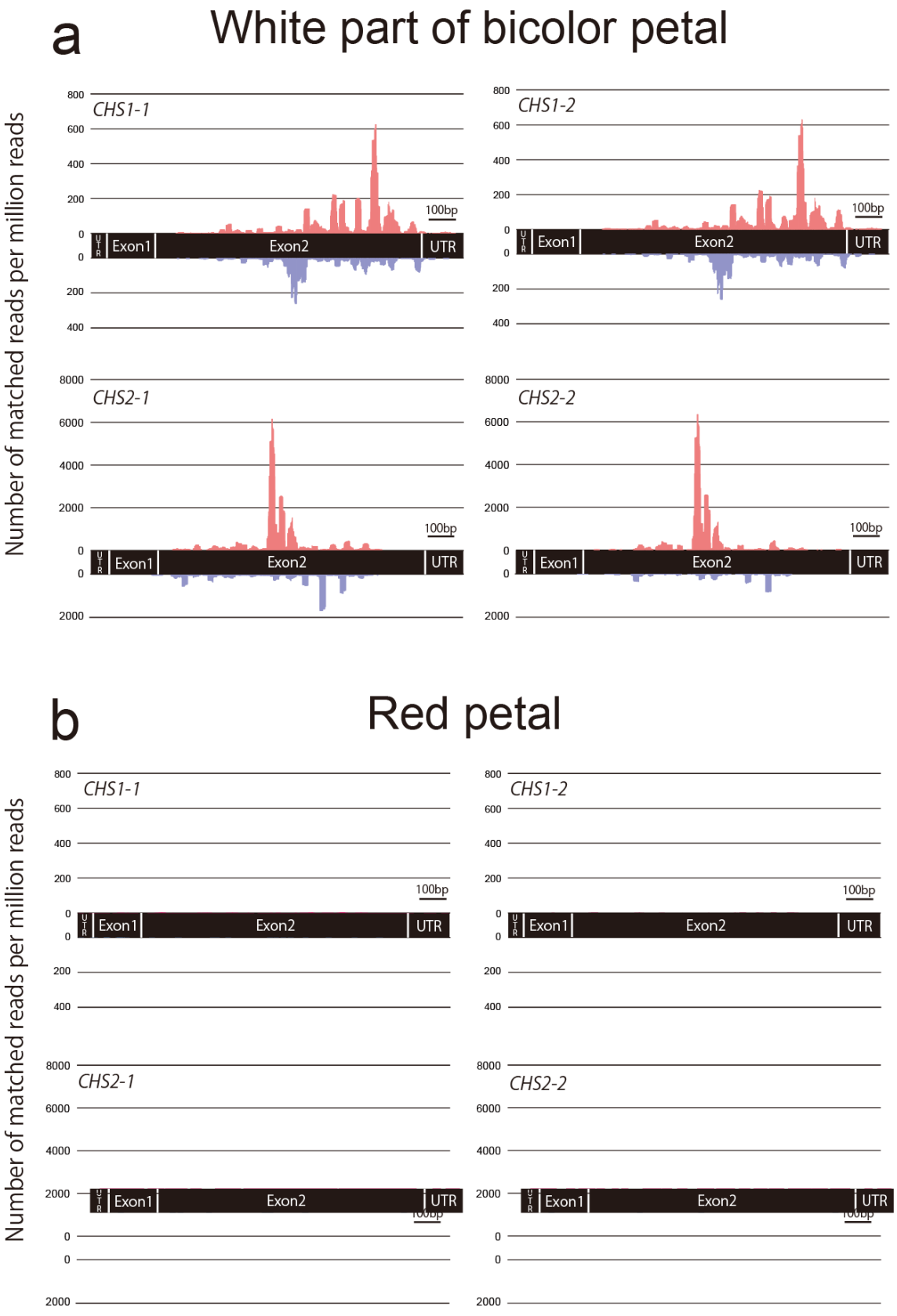

934

935 **Fig. 8**

936

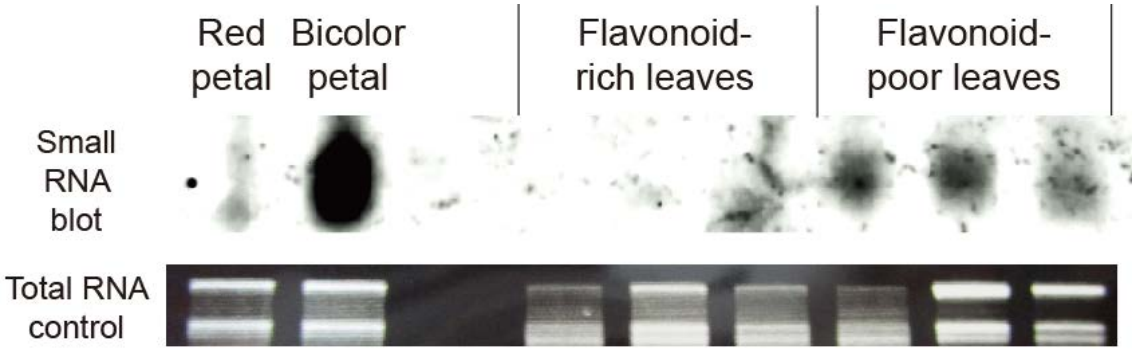

937

938

939 **Fig. 9**

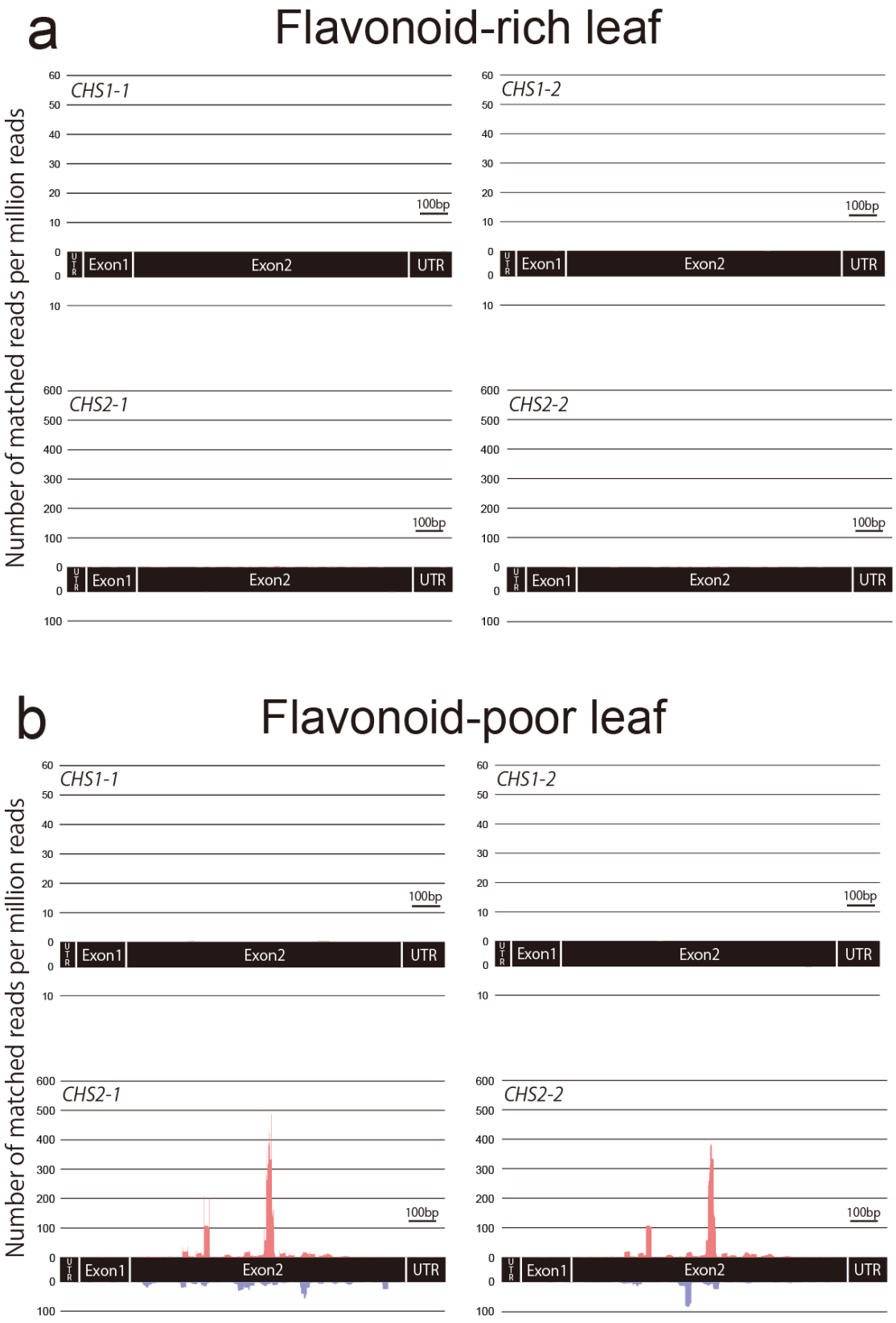

940

941 **Fig. 10**

942

943

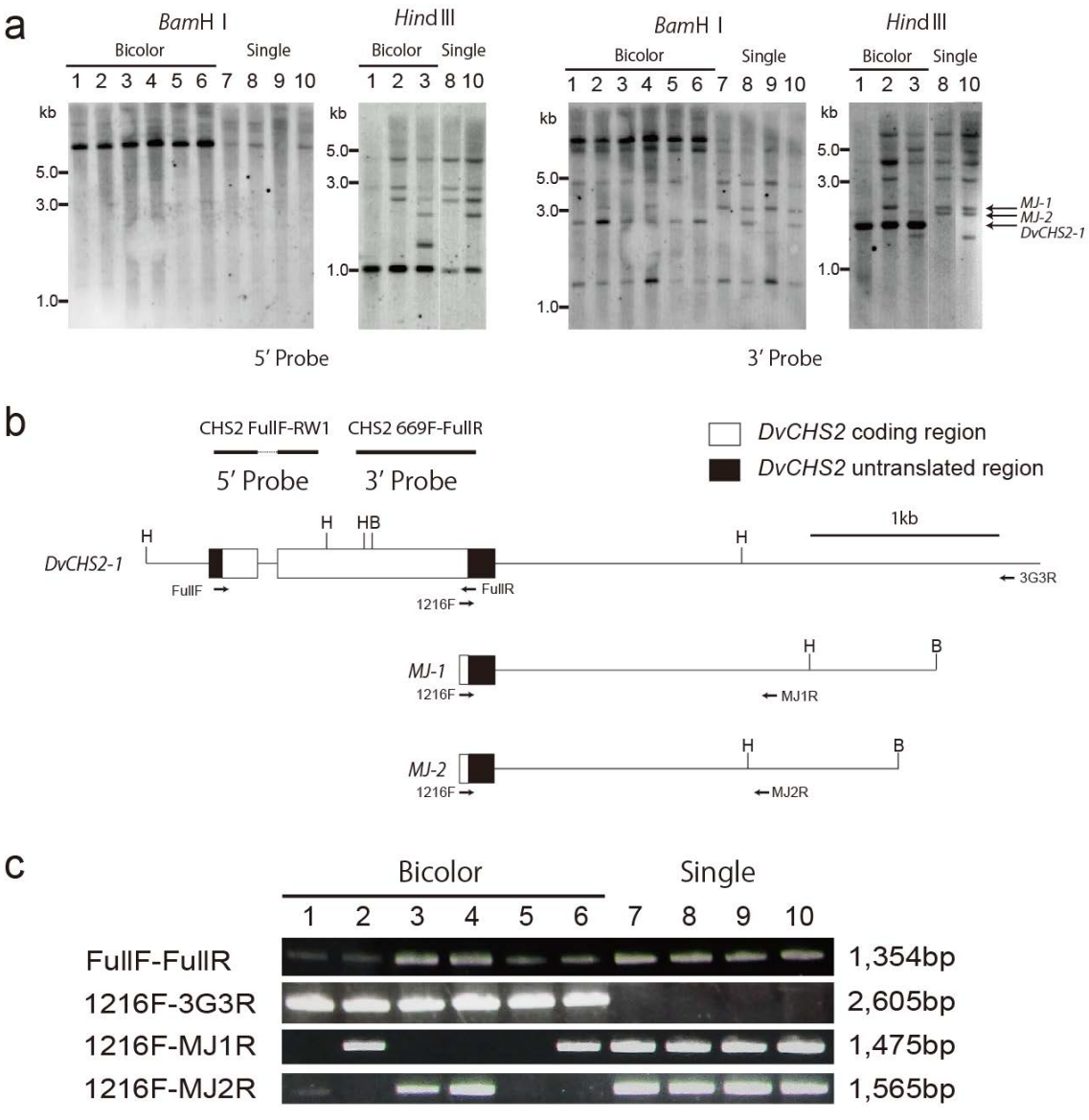

944

945

946 **Fig. 11**

947

948

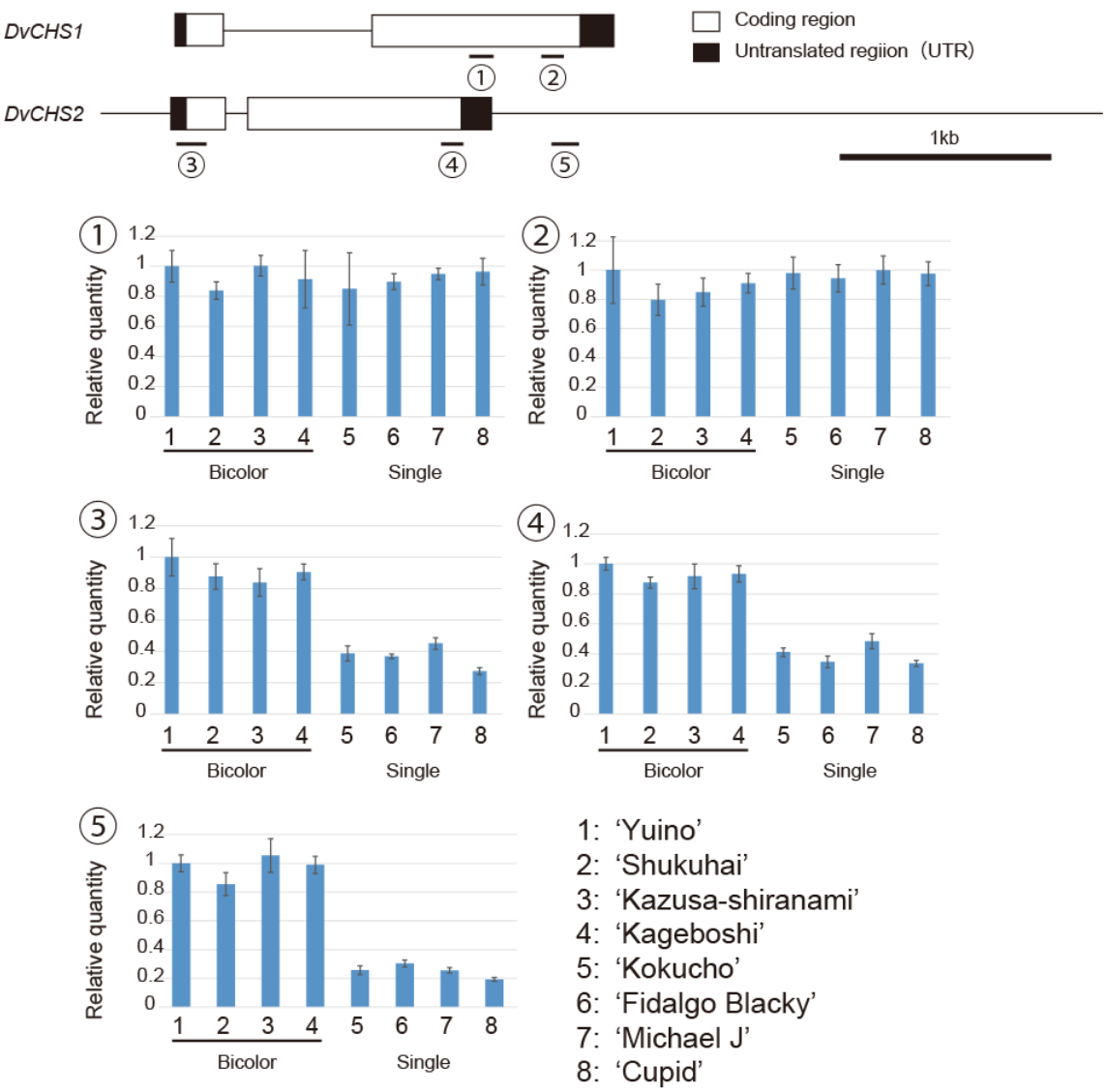

949

950

951

952

953

954

955

956 **Supplemental materials**

957 **Table S1.** Primers used for the isolation of *DvCHS3* and *DvCHS4*.

958 **Table S2.** Primers used for real-time RT-PCR.

959 **Table S3.** Primers used for identification of the *DvCHS2* flanking region.

960 **Table S4.** Primers used for qPCR for genomic quantification.

961 **Table S5.** Genes that showed significantly different expression levels between a
962 flavonoid-rich leaf and a flavonoid-poor leaf in *Dahlia variabilis* 'Yuino'.

963 **Table S6.** Top 80 most highly abundant small RNAs for which the number of total reads
964 per million (RPM) was over 1000 in a red petal and the white part of a bicolor petal of
965 *Dahlia variabilis* 'Yuino'.

966 **Fig. S1.** Genome structure of *DvCHS1–DvCHS4*.

967 **Fig. S2.** Mapping of chalcone synthase (*CHS*) small RNAs from petals onto *DvCHS3* and
968 *DvCHS4*.

969 **Fig. S3.** Mapping of chalcone synthase (*CHS*) small RNAs from leaves onto *DvCHS3*
970 and *DvCHS4*.

971

Supplemental Figure legends

Fig. S1. Genome structure of *DvCHS1–DvCHS4*. From the start codon to the stop codon was indicated. Each gene has the same conserved exon-intron junction.

Fig. S2. Mapping of chalcone synthase (*CHS*) small RNAs from petals onto *DvCHS3* and *DvCHS4*. a, white part of a bicolor petal. b, a red petal; Small RNAs of 18–32 nt with a 100% match to *DvCHS3-1*, *DvCHS3-2* or *DvCHS4* were mapped onto either the sense (above the *x*-axis) or antisense (below the *x*-axis) strand. The number of total reads of 18–32 nt was 17,455,041 for the white part of a bicolor petal and 13,681,764 for a red petal.

Fig. S3. Mapping of chalcone synthase (*CHS*) small RNAs from leaves onto *DvCHS3* and *DvCHS4*. a, a flavonoid-rich leaf; b, a flavonoid-poor leaf. Small RNAs of 18–30 nt with a 100% match to *DvCHS3-1*, *DvCHS3-2* or *DvCHS4* were mapped onto either the sense (above the *x*-axis) or antisense (below the *x*-axis) strand. The number of total reads of 18–30 nt was 12,046,092 for a flavonoid-rich leaf and 11,465,948 for a flavonoid-poor leaf.

988 **Table S1**

989

990

Table S1 Primers used for the isolation of *DvCHS3* and *DvCHS4*.

Gene	Purpose	Name	Orientation	sequence (5'-3')
DvCHS3	Race	CHS3 3'Race	sense	GTGCTCCGCAGGAGGCATGGTCCTT
	Race	CHS3 3'Race nested	sense	GGCTCGCGTGTACTTGTTGTCTGCT
	Race	CHS3 5'Race	antisense	GCACGCGCCTACTCGCCCTCAACTT
	Race	CHS3 5'Race nested	antisense	CAGCTCCACCTCGTCGAGTATGCGT
	Race	CHS3 3'Race-Re	sense	CACGTTGATTCTTTGGTCGGCCAAG
	Race	CHS3 3'Race-1	sense	GGTCTACGTGACTGGAATTCGATGT
	Sequence	CHS3 Full-F	sense	ACACATTCTTCAATAGATCAAGTTA
	Sequence	CHS3 Full-R	antisense	TTACTTATTAATTTACTACCAATCA
	Sequence	CHS3 Full-R2	antisense	CATTATTACATCAACCGTTACTTAT
	Sequence	CHS3-178F	sense	CAACGACCATATGATTGATCTTAAA
	Sequence	CHS3-446R	antisense	TTCCGGATGTGGTGCAAAAGATGAG
DvCHS4	Race	CHS4 3'Race	sense	TGGCTCGGTCCTTCGTTTGGCCAAA
	Race	CHS4 3'Race nested	sense	TTTTGGGTTGCGCATCCGGGTGGCC
	Race	CHS4 5'Race	antisense	ACCGAAGGATTAAGATCCAGGAGTT
	Race	CHS4 5'Race nested	antisense	CAATATCTCTTCGGTTAAGTACATG
	Sequence	CHS4 Full-F	sense	CACCACATACAAATTGTAACTTCAC
	Sequence	CHS4 Full-R	antisense	GTATGAAATTTCATATTATGTAATA
	Sequence	CHS4 163F	sense	AAAAAGTGAGCATATGAAGGAGCTC
	Sequence	CHS4 Int 1R	antisense	TCATTAAGAAACTAAAAAAGCCCAA
	Sequence	CHS4 Int 1F	sense	CACGGTTCAATGATAACTTACAAAG
	Sequence	CHS4 Int 2R	antisense	CTTATTCCAATTTTGAACTTTTG

991

992

993 **Table S2**

994

995

Table S2. Primers used for real-time RT-PCR.

Genes	Forward primers	Reverse primers
DvCHS1	CATGTGCTAAGCGAATACGG	CCTCTCCGGTGGTATTGAAC
DvCHS2	TGTCCCAACTACCATGCCGATTTC	TTACACATTAAAATGACACAGTGA
DvCHS3	CACCGGTGAAGGTTTAGATTGGGGT	CATTATTACATCAACCGTTACTTAT
DvCHS4	TTGGTATGCCCTATTTTCATCATGC	AAATTACATGAACAAAACATGTTT
DvCHI	AGAAGCTGGGAATGCAGTGT	GAGATCTGAGAGCCTTGATGC
DvF3H	TTGGAGGGAGATTGTGACCT	GGCCCATTAACTCCTTGCTA
DvDFR	CAACTTCCGGTCTATGACGAG	TTTCGGCCAATGTTTTTGAC
DvANS	GCTCCAACTCTTCTACAACG	GAAATCCTGACCTTCTCCTT
DvGT	AAACATCACCCTTCTTACTCT	TTGAAAAGCGCGATGGATGTT
Dv3MaT	AAATACGAAGTTGTTTCAATC	TTGCACTTTCTAATCCATCAT
DvGST	ATGTGGTGGGATGATATTTCAAACA	AACATTTATTTGTGAGTCACATACA
DvF3'H	GTAGTTATACGCAATATGCTC	CATAACTGCCTTACTATTGTAC
DvFNS	GTGTGTTTCCCTTTGCTTCGTAAAA	GCGAAGGGAAACACACTAGATTCGT
DvMYB1	GTTCACTACTTTAGCAAACG	GACTTTGATATCAACCGGAT
DvDEL	ATCTAAGTTAAAGAGTTGTACAGC	TGAAACTTGGAAAATTGGACTCAA
DvIVS	CATAACCCAAGTAAAGAAAGCCATT	CATCCATTTTTAAATTGTTTGTGGT
DvWDR1	AGGCGTTGTGGAAACTCAAT	TTATCGCGAAGGTCGAAAAC
DvActin	TGCTTATGTTGGTGATGAAG	CCCTGTTAGCCTTAGGATTT

996

997

998

999 **Table S3**

1000

1001

Table S3. Primers used for identification of the *DvCHS2* flanking region.

Cultivar	Target region	Purpose	Name	Sequence (5'-3')
Yuino	CHS2 5' flanking region	Inverse PCR-F	CHS2-3'Race-nested	GCTCGGTAAAGATGCGGCTGTCAAA
		Inverse PCR-R	CHS2 Right Walk-2	CCACGTCCTGACGGGCGTCCAAAGA
	CHS2 3' flanking region	Inverse PCR-F	CHS2 1146F	AAGGTTTGGATTGGGGTGTTCTGTT
		Inverse PCR-R	CHS2 924R	GGCGAAAACGCTTGCACCAACGCCT
		Inverse PCR-2nd-F, Sequencing	CHS2 3'Genome 6F	AATGTAATTGTCTATTTTGTTCTCT
		Inverse PCR-2nd-R	CHS2 762R	CGCTCAGTTGTCAAGTCC
		Sequencing	CHS2 3'Genome 1F	GTTGTGTTGTATGGTTCTGCTTTCT
		Sequencing	CHS2 3'Genome 2F	CCGGAGGTGCCACGCGGGGCCTTTT
		Sequencing	CHS2 3'Genome 3F	CGTGGCAATTAAACACGTTCACCT
		Sequencing	CHS2 3'Genome 4F	TCGCAAGATAATTCACGCGTGGCAA
		Sequencing	CHS2 3'Genome 5F	AGATCATAAGCGGGACG
		Sequencing	CHS2 3'Genome 7F	TCCGGCGTGAGAATCAGTATACAA
		Sequencing	CHS2 3'Genome 8F	TTGTTTTTGCGGGATGACGTCATGT
		Sequencing	CHS2 3'Genome 9F	TCACGCAAGTTCATCCGTTGGGGAT
		Sequencing	CHS2 3'Genome 1R	GGAGAAGAAAGAACAAGAAGAAAAC
		Sequencing	CHS2 3'Genome 2R	AACAGTTGACCCGACACATTCATAT
		Sequencing, allele-specific PCR	CHS2 3'Genome 3R	GGAAACACAAAATGTGTCAAAAACT
		Sequencing	CHS2 3'Genome 4R	CCTCACGCGCACCATCCCCAACGG
		Sequencing	CHS2 3'Genome 5R	AATACCAAACCCCATCATACGGTAA
		Sequencing	CHS2 3'Genome 6R	ACTAAGGACGGACGCAGCGGAACC
		Sequencing	CHS2 3'Genome 7R	GGAGCACCAGCCATTCTTGAAAAAT
		Sequencing	CHS2 3'Genome 8R	ATGGAGGAAGCATTGTTAATTAGT
Michael J	CHS2 3' flanking region	Inverse PCR-F, allele-specific PCR	CHS2-1216F	TGTCCCAACTACCATGCCGATTTC
		Inverse PCR-R	CHS2 762R	CGCTCAGTTGTCAAGTCC
		Sequencing	CHS2-Inv-MJR-Bam-Clone1-1R	GAGGGATATAAGTTTGATAAACTT
		Sequencing	CHS2-Inv-MJR-Bam-Clone2-1R	TATATGCTGTATGACTATAGTAGA
		Sequencing, allele-specific PCR	CHS2-Inv-MJR-Bam-Clone1-2R	TAACCAAGGGGGAGTGTTATAAA
		Sequencing, allele-specific PCR	CHS2-Inv-MJR-Bam-Clone2-2R	AGATTGATTAACAATCGAAGTTA

1002

1003

1004 **Table S4**

1005

1006

Table S4. Primers used for qPCR for genomic quantification.

Genes	Forward primers	Reverse primers
*DvCHS1*①	GGTGACGGTGCAGCCGCGATCAT	CGCGCCTCCACTATCCGGTAGAATA
*DvCHS1*②	CATGTGCTAAGCGAATACGG	CCTCTCCGGTGGTATTGAAC
*DvCHS2*③	TCTTATTACTGCTCGCAATATCTT	GGCGGGGTTGCAGTGCCGATGGCAA
*DvCHS2*④	AAGGTTTGGATTGGGGTGTTCTGTT	AGTTAGGGCGAAATCGGCATGGTA
*DvCHS2*⑤	TCGCAAGATAATTCACGCGTGGCAA	ATGGAGGAAGCATTGTTAATTAGT

1007

1008

1009

Table S5

Table S5. Genes that showed significantly different expression levels between a flavonoid-rich leaf and a flavonoid-poor leaf in *Dahlia variabilis* 'Yuino'.

	logFC	logCPM	FDR	ID	Description by Blastx
Up-regulated in flavonoid-rich leaf	4.10	10.08	0.001	c15993_g1	Yuino CHS2-1 (*Dahlia pinnata*) (AB591825)
	3.65	6.19	0.031	c13892_g2	PREDICTED: 23 kDa jasmonate-induced protein-like (*Malus domestica*)
Up-regulated in flavonoid-poor leaf	-5.23	4.25	0.031	c15904_g1	BTB and TAZ domain protein 1 (*Arabidopsis thaliana*) (NP201121)
	-4.33	4.77	0.031	c15650_g1	transcription factor bHLH35 (*Arabidopsis thaliana*) (NP568850)
	-4.23	7.01	0.002	c15638_g1	RESPONSE TO LOW SULFUR 2 (*Arabidopsis thaliana*) (NP197854)
	-4.01	5.17	0.031	c15986_g1	sugar transporter ERD6-like 16 (*Arabidopsis thaliana*) (NP568367)
	-3.65	8.09	0.012	c19320_g2	5'-adenylylsulfate reductase 1 (*Arabidopsis thaliana*) (NP192370)

Table S6

Table S6. Top 80 most highly abundant small RNAs for which the number of total reads per million (RPM) was over 1000 in a red petal and the white part of a bicolor petal of *Dahlia variabilis* 'Yuino'.

Sequence	Length	Description	RPM Sum	Red petal		White part of a bicolor petal	
				Read count	RPM	Read count	RPM
TTCCACGGCTTTCTTGAACTG	21		34836	446180	32611	38835	2225
TCGGACCAGGCTTCATTCCCC	21	miR165	28151	364709	26657	26077	1494
GGTTTCATTGTCACTTGACTG	21		10472	142327	10403	1204	69
CTGGATTATGACTGAACGCCT	21		4850	66081	4830	349	20
ATTCAGACGCTATGAACCATTAAG	24		3671	244	18	63768	3653
TTTGGATTGAAGGGAGCTCT	20	miR159a	3522	7653	559	51719	2963
GTTGAGGGCACGTCTGCCTGGGCGTCACG	30		3204	15345	1122	36352	2083
TCATACACCTTTCCAAATCCGC	22		3029	700	51	51982	2978
TCTCGGACCAGGCTTCATTCT	21		2925	37791	2762	2841	163
CAATGTAGGCAAGGGAAGTCG	21		2642	98	7	45984	2634
TTGAGGGCACGTCTGCCTGGGCGTCACGC	29		2596	4091	299	40100	2297
CAGAATCCGGGCTAGAAGCGA	21		2471	31129	2275	3424	196
TTCAACATCTGATCATACACC	21		2354	27948	2043	5438	312
GCGACCCCAGGTCAGGCGGGACT	23		2288	31133	2276	218	12
TAAAACGACTCTCGGCAACGGATATCTC	28		2132	8987	657	25745	1475
TTCGTTGTCTGTTCGACCTTG	21		2114	5320	389	30108	1725
AAAGAAGAACTTTGATGACGG	21		2065	58	4	35963	2060
AGTTACTAATTCATGATCTGGC	22		2047	22575	1650	6937	397
TGGATTGTGCTGCATCGTCTG	21		2005	371	27	34519	1978
TCGGACCAGGCTTCATTCCTC	21		1991	17630	1289	12267	703
GCCCGCGACGTCGCGAGAATTCCACTGAAC	32		1952	26559	1941	188	11
TGGAACAATGTAGGCAAGGGAAGTCGGCA	29		1893	16	1	33018	1892
AGATTCAGCCCTGCGTCGCTCAGATTCGT	29		1890	25510	1865	451	26
GTTCGAGAAAACTGTGGGAAA	21		1853	5965	436	24730	1417
TGAAGCTGCCAGCATGATCTG	21	miR167	1793	1230	90	29722	1703
TAAAACGACTCTCGGCAACGGATATC	26		1718	9966	728	17278	990
AACGACTCTCGGCAACGGATATCTCGGCT	29		1717	21607	1579	2408	138
TAAAACGACTCTCGGCAACGGA	22		1688	18100	1323	6374	365
CATAGTAGCCAAGGAAGACGA	21		1640	57	4	28555	1636
TGGACCGACGGATACTCATCT	21	*DvCHS2*	1624	0	0	28351	1624
CCAGGGATCAGCGGATGTTGC	21		1605	21847	1597	139	8
CAAGTGACAATGAAACCGCCT	21		1594	21718	1587	119	7
TTGTGACGAAGATGGCGAGAA	21		1561	4498	329	21507	1232
TAAAACGACTCTCGGCAACGGATATCTCGG	31		1528	3526	258	22175	1270
TAAAACGACTCTCGGCAACG	20		1524	15013	1097	7448	427
AGTTAAAAAGCTCGTAGTTGGACC	24		1502	19781	1446	987	57
TTTGGATTGAAGGGAGCTCTA	21	miR159a	1453	4474	327	19656	1126
TTTAAGAAGATGGAACGTCAG	21	*DvCHS2*	1451	0	0	25320	1451
GCAGTTAAAAAGCTCGTAGTTGGACC	26		1441	18803	1374	1169	67
TGGAACAATGTAGGCAAGGGAAGTCGGC	28		1407	18	1	24533	1405
ATGGAACAATGTAGGCAAGGGAAGTCGGCA	30		1399	1399	102	22637	1297
TTTCGGACCAGGCTTCATTCC	21	miR166n	1366	18584	1358	143	8
GATGGAACAATGTAGGCAAGGGAAGTCGG	31		1357	325	24	23264	1333
CAAGCTTTGTTTGGGGACGGT	21	*DvCHS2*	1343	0	0	23436	1343
TGGAACAATGTAGGCAAGGGAAGTCGG	27		1342	7	1	23424	1342
ATCCGGTTAGGATCGATCTAAACCAGCC	28		1329	13294	972	6235	357
AGAAACGATTGTCCTTACTTT	21		1327	17798	1301	459	26
TGACAGAAGAGAGTGAGCAC	20	miR156a	1313	2525	185	19689	1128
TTCCACAGCTTTCTTGAACTT	21		1283	16903	1235	837	48
TTTGCACTTTTGATATCACGG	21		1278	3589	262	17721	1015
TGCAAGAGGGCTTGAACACGG	21		1269	30	2	22107	1267
TTAAAGCTTAGAAAAACGTCGT	22		1262	745	54	21075	1207
CACGAACTTTGATATCTAGGC	21		1260	382	28	21502	1232
AACGACTCTCGGCAACGGATATC	23		1241	14076	1029	3700	212
TCTGAACAGAAGATGGACCACC	22		1233	305	22	21127	1210
TAAAACGACTCTCGGCAACGGATATCTCGG	32		1226	8756	640	10226	586
GAGAGACCTATTAACGAGCCT	21		1222	16693	1220	37	2
TGGAACAATGTAGGCAAGGGAAGTCGGCA	30		1215	5	0	21200	1215
CTCTAAGTCAGAATCCGGGCT	21		1176	16047	1173	49	3
TTTGATGGATACGAAGAGAAG	21		1171	791	58	19431	1113
TTGCAGTTAAAAAGCTCGTAGTTGGACC	28		1138	15021	1098	701	40
GATGGAACAATGTAGGCAAGGGAAGTCGG	30		1126	97	7	19539	1119
TCCATTGTCGTCCAGCGGTTAGGATA	26		1108	14793	1081	472	27
CAGAAGACTCAGCTCGCTCCT	21		1095	8263	604	8578	491
TGGAACAATGTAGGCAAGGGAAGTCGGCA	31		1087	9	1	18968	1087
CAATGTAGGCAAGGGAAGTCGG	22		1059	20	1	18468	1058
CGTGGACCGACGGATACTCAT	21	*DvCHS2*	1059	0	0	18482	1059
ATCCGGTTAGGATCGATCTAAACCAGCCC	29		1052	12339	902	2626	150
TTAAAGAAGAACTTTGATGAC	21		1050	13	1	18311	1049
CGGATACTCATCTTGATTCGC	21	*DvCHS2*	1039	0	0	18129	1039
TAAAACGACTCTCGGCAACGG	21		1035	6294	460	10043	575
TAAAACGACTCTCGGCAACGGATATCT	27		1033	3520	257	13547	776
TTCCGAGCCTACCGATTCCAGC	22		1033	3514	257	13543	776
GAGATTCAGCCCTGCGTCGCTCAGATTCGT	30		1033	13918	1017	269	15
TGGAACAATGTAGGCAAGGGAAGTCGGCA	32		1028	8	1	17930	1027
ATGGAACAATGTAGGCAAGGGAAGTCGGC	29		1021	231	17	17532	1004
GGGGATGTAGCTCAGATGGT	20		1015	1278	93	16083	921
TTAAAGAAGAACTTTGATGACG	22		1014	58	4	17622	1010
CAACAAGGCTGTAGCGAGGGC	21		1009	1323	97	15921	912
CAGTTAAAAAGCTCGTAGTTGGACC	25		1008	13077	956	919	53

Total read of red petal and the white part of the bicolor petal was 13,681,764 and 17,455,041, respectively.

Fig. S1

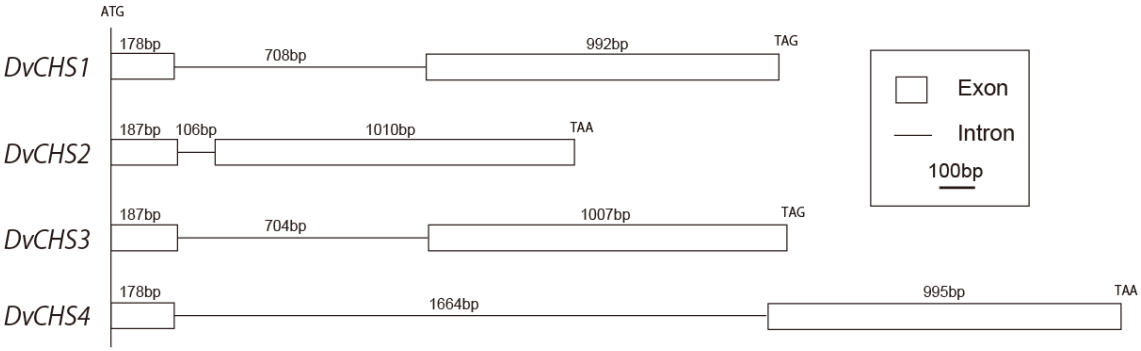

1037 **Fig. S2**

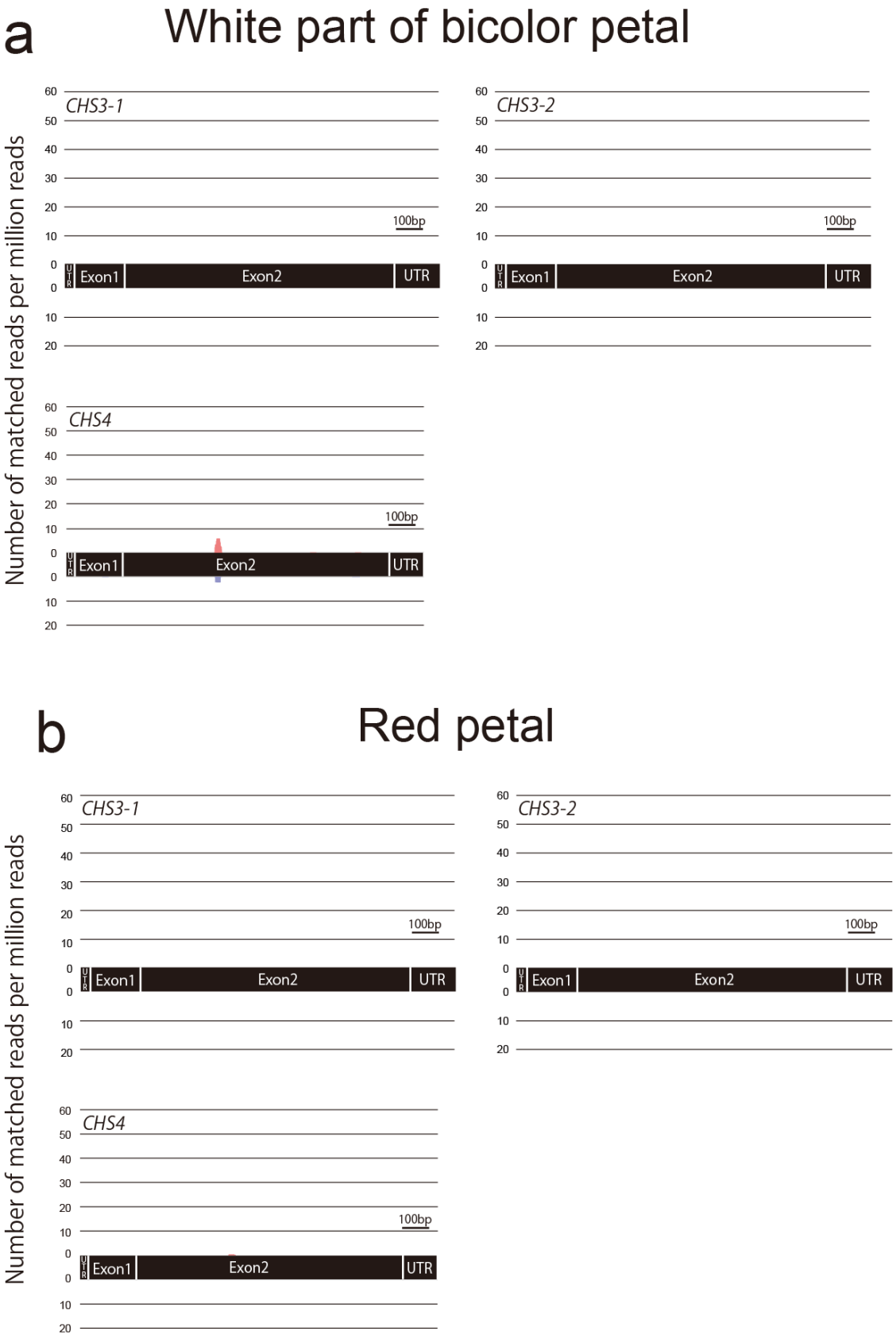

1038

1039 **Fig. S3**

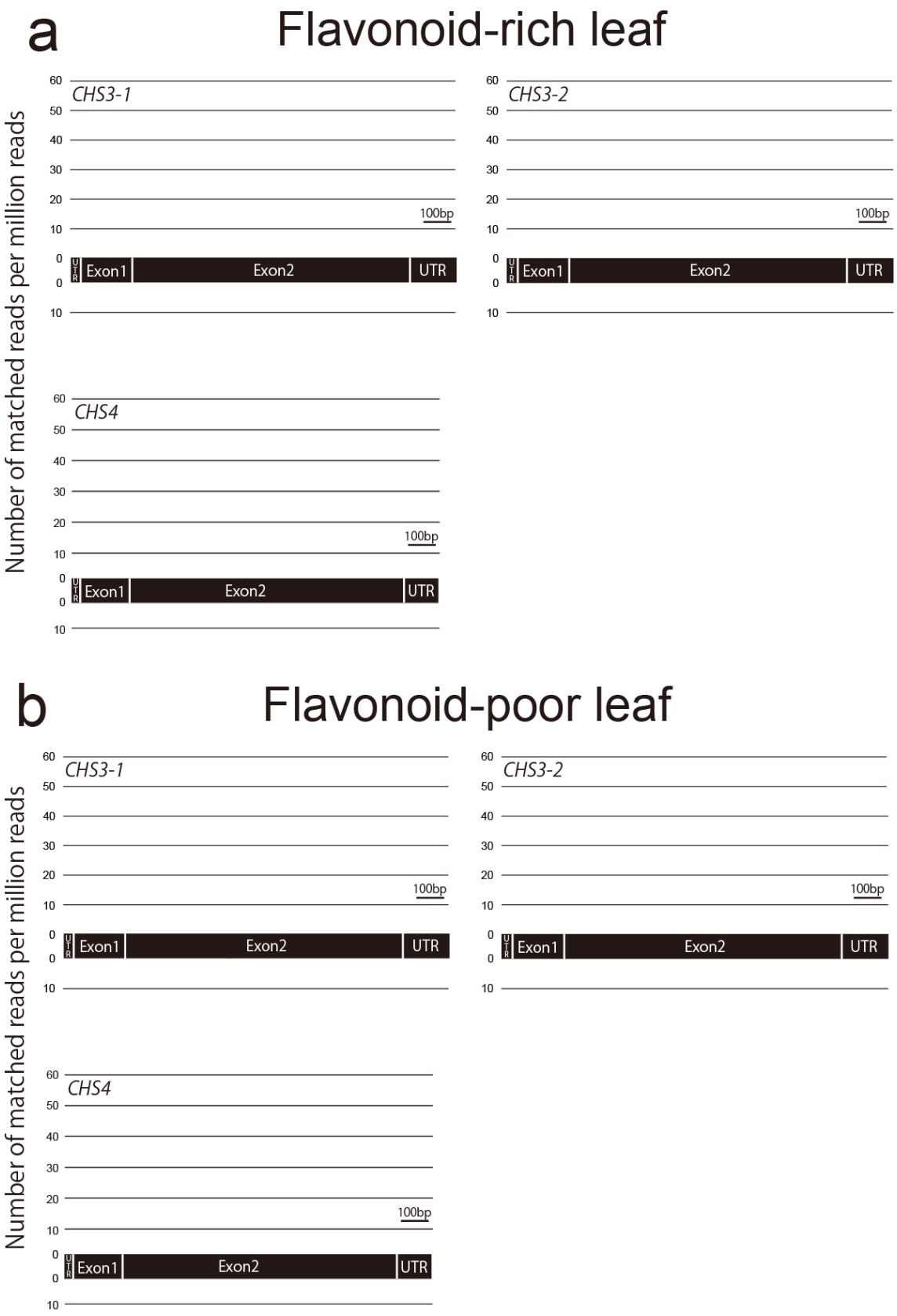

1040

1041